UNIVERSIDADE DE LISBOA
FACULDADE DE CIÊNCIAS
DEPARTAMENTO DE INFORMÁTICA

Implementation of an hybrid machine learning methodology for pharmacological modeling

Katarzyna Malgorzata Kwiatkowska

DISSERTAÇÃO
MESTRADO EM BIOINFORMÁTICA E BIOLOGIA COMPUTACIONAL
ESPECIALIZAÇÃO EM BIOINFORMÁTICA

Dissertação orientada por:
Prof. Andre Osorio Falcão
Prof. Lisete Maria Ribeiro de Sousa

2017

Resumo

Hoje em dia, especialmente na área biomédica, os dados contêm milhares de variáveis de fontes diferentes e com apenas algumas instâncias ao mesmo tempo. Devido a este facto, as abordagens da aprendizagem automática enfrentam dois problemas, nomeadamente a questão da integração de dados heterogéneos e a seleção das características. Este trabalho propõe uma solução eficiente para esta questão e proporciona uma implementação funcional da metodologia híbrida. A inspiração para este trabalho veio do desafio proposto no âmbito da competição AstraZeneca-Sanger Drug Combination Prediction DREAM Challenge em 2016, e da solução vencedora desenvolvida por Yuanfang Guan. Relativamente a motivação do concurso, é observado que os tratamentos combinatórios para o cancro são mais eficientes do que as terapias habituais de agente único, desde que têm potencial para superar as desvantagens dos outros (limitado espetro de ação e desenvolvimento de resistência). No entanto, o efeito combinatório de drogas não é obvio, produzindo possivelmente o resultado aditivo, sinérgico ou antagónico. Assim, o objetivo da competição era prever in vitro a sinergia dos compostos, sem ter acesso aos dados experimentais da terapia combinatória. No âmbito da competição foram fornecidos ficheiros de várias fontes, contendo o conhecimento farmacológico tanto experimental como obtido de ajustamento das equações, a informação sobre propriedades químicas e estruturais de drogas, e por fim, os perfis moleculares de células, incluindo expressão de RNA, copy variants, sequência e metilação de DNA. O trabalho referido envolveu uma abordagem muito bem sucedida de integração dos dados heterogéneos, estendendo o modelo com conhecimento disponível dentro do projeto The Cancer Cell Line Encyclopedia, e também introduzindo o passo decisivo de simulação que permite imitar o efeito de terapia combinatória no cancro. Apesar das descrições pouco claras e da documentação da solução vencedora ineficiente, a reprodução da abordagem de Guan foi concluída, tentando ser o mais fiel possível. A implementação funcional foi escrita nas linguagens R e Python, e o seu desempenho foi verificado usando como referência a matriz submetida no concurso. Para melhorar a metodologia, o workflow de seleção dos características foi estabelecido e executado usando o algoritmo Lasso. Além disso, o desempenho de dois métodos alternativos de modelação foi experimentado, incluindo Support Vector Machine and Multivariate Adaptive Regression Splines (MARS). Várias versões da equação de integração foram consideradas permitindo a determinação de coeficientes aparentemente ótimos. Como resultado, a compreensão da melhor solução de competição foi desenvolvida e a implementação funcional foi construída com sucesso. As melhorias foram propostas e no efeito o algoritmo SVM foi verificado como capaz de superar os outros na resolução deste problema, a equação de integração com melhor desempenho foi estabelecida e finalmente a lista de 75 variáveis moleculares mais informativas foi fornecida. Entre estes genes, poderiam ser encontrados possíveis candidatos de biomarcadores de cancro.

Palavras Chave: aprendizagem automática, modelo preditivo, seleção de características, integração de dados

Abstract

Nowadays, especially in the biomedical field, the data sets usually contain thousands of multi-source variables and with only few instances in the same time. Due to this fact, Machine Learning approaches face two problems, namely the issue of heterogenous data integration and the feature selection. This work proposes an efficient solution for this question and provides a functional implementation of the hybrid methodology. The inspiration originated from the AstraZeneca-Sanger Drug Combination Prediction DREAM Challenge from 2016 and the winning solution by Yuanfang Guan. Regarding to the motivation of competition, the combinatory cancer treatments are believed to be more effective than standard single-agent therapies since they have a potential to overcome others weaknesses (narrow spectrum of action and development of the resistance). However, the combinatorial drug effect is not obvious bringing possibly additive, synergistic or antagonistic treatment result. Thus, the goal of the competition was to predict in vitro compound synergy, without the access to the experimental combinatory therapy data. Within the competition, the multi-source files were supplied, encompassing the pharmacological knowledge from experiments and equation-fitting, the information on chemical properties and structure of drugs, finally the molecular cell profiles including RNA expression, copy variants, DNA sequence and methylation. The referred work included very successful approach of heterogenous data integration, extending additionally the model with prior knowledge outsourced from The Cancer Cell Line Encyclopedia, as well as introduced a key step of simulation that allows to imitate effect of a combinatory therapy on cancer. Despite unexplicit descriptions and poor documentation of the winning solution, as accurate as possible, reproduction of Guan's approach was accomplished. The functional implementation was written in R and Python languages, and its performance was verified using as a reference the submitted in challenge prediction matrix. In order to improve the methodology feature selection workflow was established and run using a Lasso algorithm. Moreover, the performance of two alternative modeling methods was experimented including Support Vector Machine and Multivariate Adaptive Regression Splines (MARS). Several versions of merging equation were considered allowing determination of apparently optimal coefficients. As the result, the understanding of the best challenge solution was developed and the functional implementation was successfully constructed. The improvements were proposed and in the effect the SVM algorithm was verified to surpass others in solving this problem, the best-performing merging equation was established, and finally the list of 75 most informative molecular variables was provided. Among those genes, potential cancer biomarker candidates could be found.

Keywords: machine learning, predictive model, feature selection, data integration

Resumo Alargado

Hoje em dia, especialmente na área biomédica, os dados contêm milhares de variáveis de fontes diferentes e com apenas algumas instâncias ao mesmo tempo. Devido a este facto, as abordagens da aprendizagem automática enfrentam dois problemas, nomeadamente a questão da integração de dados heterogéneos e a seleção das características. Este trabalho propõe uma solução eficiente para esta questão e proporciona uma implementação funcional da metodologia híbrida. A inspiração para este trabalho veio do desafio proposto no âmbito da competição AstraZeneca-Sanger Drug Combination Prediction DREAM Challenge em 2016, e da solução vencedora desenvolvida por Yuanfang Guan. Relativamente a motivação do concurso, é observado que os tratamentos combinatórios para o cancro são mais eficientes do que as terapias habituais de agente único, desde que têm potencial para superar as desvantagens dos outros (limitado espetro de ação e desenvolvimento de resistência). No entanto, o efeito combinatório de drogas não é obvio, produzindo possivelmente o resultado aditivo (se o resultado é equivalente aos efeitos somados de dois medicamentos), sinérgico (quando a resposta é exagerada e superior dos efeitos aditivos de dois produtos químicos) ou antagónico (com uma resposta inferior do efeitos somados do par de drogas). Assim, o objetivo da competição era prever in vitro a sinergia dos compostos, sem ter acesso aos dados experimentais da terapia combinatória. No âmbito da competição foram fornecidos ficheiros de várias fontes, contendo o conhecimento farmacológico tanto experimental como obtido de ajustamento das equações, a informação sobre propriedades químicas e estruturais de drogas, e por fim, os perfis moleculares de células, incluindo expressão de RNA, copy variants, sequência e metilação de DNA. O trabalho referido envolveu uma abordagem muito bem sucedida de integração dos dados heterogéneos, estendendo o modelo com conhecimento disponível dentro do projeto The Cancer Cell Line Encyclopedia. No entanto, os dados moleculares são inúteis a menos que sejam simulados sob a droga, imitando o efeito de uma terapia combinatória em células. Yuanfang Guan propôs uma abordagem baseada no conhecimento disponível na base de dados Functional Networks of Tissues in Mouse (FNTM) e resumida no ficheiro externo contendo informações sobre as rede funcionais entre os genes e a probabilidade destas conexões. A ideia principal era alterar cada estado original atribuído às células cancerosas, de acordo com a probabilidade de ligação entre dois genes: o gene em consideração e o gene alvo para a droga aplicada. De acordo com a implementação original, todas as fontes moleculares foram filtradas e exclusivamente o conhecimento relacionado com o conjunto dos alvos foi considerado. Para produzir as previsões finais, foram construídos seis modelos: dois globais de dados moleculares e de monoterapia, um químico, um contando ficheiros, e mais dois locais de dados moleculares e de monoterapia. Os nomes deles indicam a fonte de dados utilizada na construção de vetores de variáveis. Posteriormente, as previsões obtidas de todos os modelos foram integradas usando média ponderada. Para determinar a ocorrência do efeito sinérgico para a combinação específica de par de drogas e da célula, as previsões produzidas foram comparadas com a média total calculada para todas as instâncias. O efeito benéfico é esperado nos casos que representam o valor normalizado da sinergia superior da média global. Apesar das descrições pouco claras e da documentação da solução vencedora ineficiente, a reprodução da abordagem de Guan foi concluída, tentando ser o mais fiel possível. A implementação funcional foi escrita nas linguagens R e Python, e o seu desempenho foi verificado usando como referência a matriz submetida no concurso. Devido ao facto que os processos computacionalmente envolvidos na manipulação de dados moleculares foram intensos, uma filtração adicional dos dados foi realizada. O objetivo era reduzir o número de variáveis selecionando unicamente as características informativas e relevantes. Baseando na informação contida na plataforma IntOGen, as mutações foram limitadas exclusivamente às localizadas nos oncogenes. A base de dados The Copy Number Variations in Disease foi usada para mapear genes de cancro sensíveis à dosagem e para selecionar os CNVs relevantes. Embora eficaz na redução do tamanho, este

passo de filtração tem o poder elevado de interferir com os dados porque limita o espaço das variáveis ao conhecimento já bem estabelecido. Assim, a inferência de potenciais correlações ou implicações está inibida. Após o desenvolvimento da implementação funcional, a precisão e fidelidade da reprodução foram estimadas verificando o desempenho usando como referência a matriz de previsões submetida no concurso. Esta proeza permitiu o estabelecimento de uma base e a definição de pontos fracos do método, que no resultado indicou direções de melhoramento. Uma vez que o número de variáveis moleculares foi um desafio real na manipulação, processamento e interpretação, foi decidido realizar a seleção de características. Ao contrário da filtração anterior, esse método abre um espaço para a inferência dos novos padrões e conexões. A importância e a relevância de uma variável são estimadas baseando nos dados experimentais que refletem o funcionamento de um sistema biológico inteiro e possivelmente nova compreensão pode ser surgir. Após várias tentativas, o workflow final foi estabelecido usando um algoritmo chamado Lasso. Em primeiro lugar, para cinco fontes de dados moleculares (exceto metilação devido ao processamento altamente intenso), os modelos foram preparados com um parâmetro λ indefinido, permitindo a observação do comportamento do erro quadrático médio (Mean Square Error, MSE) em função de lambda. A inspeção visual de gráfico permitiu a estimativa de λ correspondente ao minimo valor de MSE. Seguindo essa abordagem, para cada uma das fontes, o parâmetro foi estimado separadamente. Voltou-se construir os modelos de lasso, mas desta vez com λ definido e em 60 iterações. Para cada fonte de dados moleculares foram selecionadas as variáveis com frequência de ocorrência superior de 30 em total das 60 corridas e posteriormente foram todas incluídas numa única lista. O passo inicial foi repetido, mas desta vez exclusivamente para as características pré-selecionadas. Encontrando o parâmetro lambda máximo para o qual o número das variáveis é igual ou inferior a 60, realizou-se uma seleção final, extraindo apenas aquelas instâncias que entram no modelo com tal λ definido. Para verificar se os RFs originalmente aplicados são verdadeiramente o método de preferência para este conjunto de dados, dois outros algoritmos de modelação foram testados: Support Vector Machine and Multivariate Adaptive Regression Splines (MARS). Uma vez que não havia qualquer tipo de referência ou evidência que justificava a forma de combinação dos modelos separados criados ao longo da implementação, foram testadas várias versões da mesma equação de integração, permitindo a determinação dos coeficientes aparentemente ótimos. Para tornar a avaliação de implementação final mais confiável, foram usados como referência os valores de sinergia verdadeiras (em vez de previstas por Yuanfang Guan). Formou-se novos conjuntos de treinamento e teste, a partir dos dados conhecidos disponíveis no âmbito de concurso. Os subconjuntos reconstruíram as circunstâncias de modelação originais, o que na prática significa que eles foram totalmente disjuntas nos pares de drogas (como os originais) e foram equilibrados por tamanho contendo, respetivamente 30% e 70% de informação. Além disso, a matriz binária de predições foi melhorada e foi feita uma distinção entre 'sem sinergia' e 'dados indisponíveis', atribuindo valores respetivamente '0' e 'NA'. Isto garantiu que a avaliação foi realizada exclusivamente nas instâncias de teste, impedindo a excessiva representação de observações verdadeiras negativas, como aconteceu durante a avaliação da implementação base. Como resultado, ao longo deste trabalho, a compreensão da melhor solução de desafio foi desenvolvida e a implementação funcional foi construída com sucesso. Foram propostas as melhorias na metodologia, em relação à seleção de características, modelação e aos passos de integração. No efeito, foi fornecida a lista de 75 variáveis moleculares de toda informação sobre expressão, mutações e CNVs. Entre estes genes, poderiam ser encontrados possíveis candidatos a biomarcadores do cancro, merecendo mais atenção e exploração. O algoritmo SVM foi verificado a superar os RFs na resolução do problema de competição, e a equação de integração com o melhor desempenho foi estabelecida. A implementação final tornou-se um exemplo da abordagem que fornece uma solução eficiente para os problemas de aprendizagem automática com os dados heterogéneos de muitas variáveis e poucas instâncias.

Acknowledgements

This work was performed with resources from research Project MIMED - Mining the Molecular Metric Space for Drug Design (PTDC/EEI-ESS/4923/2014), sponsored by FCT - Fundação para a Ciência e a Tecnologia.

In the first place I would like to thank to my both master thesis supervisors: Prof. André Osorio Falcão and Prof. Lisete Maria Ribeiro de Sousa. Without the doubt, this work would never be accomplished if not their support. I am especially grateful for their acceptance and openness to my curiosity, and for allowing me to explore the Unknown on my way. Being guided by them through the Science is a huge honour and a pleasure for me.

I am especially grateful to Prof. Lisete Maria Ribeiro de Sousa for her trust in me and confidence in my skills. For infinite patience, the extraordinary positive attitude and a bright smile - that is what I really wish to thank her for.

After first week of putting hands on this project Prof. André asked me if I had fun. Indeed I had. Not only during the first week but over all this time. For this priceless lesson, I want to express my special gratitude.

Further, to my main advisor, I would like to thank for the never-ending and contagious enthusiasm, for the understanding beyond the words, and finally for the absolutely right words in the exact moment.

I wish to acknowledge also my previous supervisor of my Master thesis in Biotechnology at University of Aveiro, António Correia. He was the person who encouraged me to ask ‘why?’ opening by this a door that I cannot close until now and hopefully will not do that never in the future.

To my LaSIGE collegues for makeing this journey together, in fabulous company. Especial thanks to Pati and Beatriz for the time and energy spend firstly on struggling trying to understand what actually is in my head, and then turning it understandable to the portuguese part of the world.

I am very thankful to my great friend, amazing and inspiring researcher, Gautam Agarwal. He must be appreciated since without him this work would be definitely missing the section with results.

Thanks to objectT for all the firmware & software updates, backups, numerous defragmentations, technical and mute support.

Finally, I wish to express my gratitude to family, friends and all those who have contributed to this work and know their own names.

this work is dedicated to Pu
one of my very best friends
fighting against the cancer
with the most beautiful smile in the world
until the end

Contents

List of Tables

List of Figures

1. Introduction

1.1. Problem

The aim of this work is to propose an efficient approach that provides a solution for machine learning problems with thousands of multi-source variables and with only few instances in the same time. Thus, there are two separate but equally interesting aspects: heterogenous data integration and feature selection.

With the recent advance in technologies, production and acquisition of a data is not an issue any more. Every day, every minute, continuously there are giga-bytes, tera-bytes of diverse information being generated [1]. The matter is how to turn it all efficiently to an useful knowledge that would truly bring a change to the world. The very first step on that pathway is a data integration that aims merging of the data provided by different sources, having particular structures and manner of organization, finally holding an information on various subjects [2]. The field of biomedical research is one of the cases which is abundant in data encompassing genomics, transcriptomics, metabolomics, proteomics and clinical records, and the efficient tools making a use of those are needed [3].

Recently a special attention has been given to the research on pattern recognition in a data with redundant and potentially irrelevant information among small set of samples [4]. All the methods targetting this challenge has a principal idea in common, that is the identification and opting for a subset of predictors [5][6]. The advantages of feature selection are numerous and unquestionable: easing the visual representation and interpretation of data, facilitating its handling and storing, turning training and querying less time- and resources-consuming, and finally achieving a better performance through effective managing with the dimensionality [7]. The approaches widely proposed in scientific literature differ in the focus, giving more attention to some aspects than to another, and one need to select a solution according to the particular objectives and the problems faced with. The main question to answer is to identify which features shall be selected: relevant or useful, because those, surprisingly, are not necessarily equal and it is crucial to understand the difference [8][9]. The set of useful variables includes only those which build good predictions, while in contrast, the list of relevant variables contains factors highly correlated with the response that usually brings the suboptimal result.

The inspiration to the present work, originated from the AstraZeneca-Sanger Drug Combination Prediction DREAM Challenge from 2016 and the winning solution provided by an excellent scientist: Yuanfang Guan. Launching the competition, several institutions joined their efforts and ideas, including AstraZeneca, European Bioinformatic Institute, the Sanger Institute, Sage Bionetworks and finally DREAM community [10]. The referred the best submission included very successful approach of heterogenous data integration encompassing among others chemical, experimental and multi-source

molecular data on RNA expression, copy variants, DNA sequence and methylation. Additionally, the author introduced a crucial simulation step that modeled the profiles of cell lines under the application of particular treatments.

Regarding to feature selection, the step was proposed and included within the optimization procedures. Beside the improvement of performance, this process allowed identification of potential molecular biomarkers that could be important in predicting the synergy under the treatment.

The acquired knowledge was also hoped to bring an insight into determination of the behavior and outcome of combinatory treatments with new compounds or new combinations and with extended application to various diseases. The drug-pairs are already widely used as therapeutics in hepatitis C virus, malaria, pneumonia, asthma and others [11]. Their potential is still not evaluated in number of clinical cases for example in neuropathologies or mood disorders.

1.2. The wisdom of crowds

"No one in this world, so far as I know, has ever lost money by underestimating the intelligence of the great masses of the plain people."
H. L. Mencken

The quotation above is wrong, as proved by Surowiecki in his book [12]. The knowledge that comes from a community is much more powerful than an individual idea. This concept became a principle of any crowdsourcing effort, likewise of the initiator DREAM Challenge. Its objective is to examine a biological and medical questions by collective approach [13]. Each year a number of problems is brought to the scientific community that joins the researches from different environments and backgrounds like academical, technological, biotechnological or pharmaceutical, including companies, non-profit organization etc [14]. The participants are always provided with datasets on which they develope their methodologies, and additionally with the common benchmarks and standardized performance metrics that allow the evaluation and comparison after the realized submissions [15].

Despite of the impressing advance in medicine and pharmacology, cancer still continues to win many fights for human lives. This is uncontrolled intense growth of cells driven by genetic factors that are interconnected in complex network of interactions. The therapies commonly applied usually target an individual cancer line and are not able to effieciently control the tumor development [16]. The combinatory cancer treatments are believed to be more effective than standard single-agent therapies since they have a potential to overcome others weaknesses. Mainly, they shall present broaden range of activity, targeting simultaneously more than a single protein or biological pathway, and they should bring a solution to a resistance gain during the medication. This boost of the anticancer activity must be achieved obviously without consequences of increased toxicity [17]. While designing such a therapy, the very first property to be taken into consideration shall be a combinatorial drug effect that eventually can be:

1) Additive, if the final result is equivalent to summed outcomes of each drug;

2) Synergistic, when the response is exaggerated and beyond the additive effects of two chemicals;

3) Antagonisitic, with a reply beneath the summed effects of drug pair.

Although the concept is simple and highly promising, it is an issue to accurately predict the combinatory effect of drugs due to the lack of explicit understanding of underlying interaction mechanisms [18]. Thus, the assessment is mainly built on experimental measurements. However, in practice and in laboratory it turns very complicated due to a very large number of possibilities of drug combinations and their dosages. For this reason, the predictive models that would bring a support, are urgently sought for and became a problem brought by a DREAM to a research community.

The shared idea that united a board of referred already challenge, was to contribute to an expansion of knowledge on synergy of drugs. Thus, the goal of competition was an exploration of crucial patterns that drive the combinatory therapies of a cancer patients, leading to a particular response. The participants were asked to determine a drug combination effects on a experimental data from mono-therapies. The main issue – how to infer a knowledge on the drug-pair synergy, basing on dose response observed for single compounds, was solved by organizers. They proposed a method able to compute the combination effects and provided the participants with both: experimental mono-therapy measurements and inferred synergy scores. The details on the introduced approach are presented in section 2.1.3. Pharmacological Data.

1.3. Work Progress

While achieving the goal of this work three keypoints were successfully completed:

1. Profund understanding of the original approach;
2. Functional reproduction of the methodology;
3. Introduction of improvements to the baseline.

There were nine main tasks realized during the accomplishment (Figure 1.1.). Firstly, the work on the project encompassed exploration and basic training on Machine Learning methods. This practice was performed on original data sets from the DREAM competition and was based on the problems brought within the subchallenge 1 and the collaborative round. Since both of them are not directly relevant to the work, the details are here omitted. While fulfilling this task, the database was organized, which served as a fundamental structure used in all following steps.

From November, the basics of the PERL programming language had been learnt. This was necessary in order to accomplish the second part of the task – familiarization with Yuanfang Guan's method. Through reading of the documents and additional resources supporting the approach, the understanding and interpretation of concept were developed.

January was dedicated to direct reading of PERL scripts. It allowed exploration of how the idea was practically implemented. The concept gain a physical structure that could be further transferred and developed in other computational environments.

Next 2 months were spend on establishing of reproduction of original version, using R and Python languages. Finally, the functional baseline implementation was successfully created and could be evaluated. From this point on, the steps performed were an adds-on applied above the baseline implementation.

In order to reflect what had been already achieved and what urges the improvement, on 28th of March 2017 the work was presented to a small audiency, including both supervisors of this work. This important revision allowed determination of a direction of the next steps. Crucial questions regarding

to missing values imputation, final test and trainig sets and optimization were decided, resulting in a defined improvement plan.

Contrary to expectations, at thas time, the true values of synergy scores in a challenge test set, still did not become available to a public. Due to this fact, the test and training sets were generated from known data, reproducing as accurately as possible the modeling conditions created in DREAM challenge.

One of the most laborious steps was the task 7 - feature selection. Different methodologies were experimented before establishing a workflow, for example Random Forests, Support Vector Machine, Generalized linear and additive models by likelihood based boosting (GAMBoost). The final result, accomplished with Lasso algorithm, provided a list of useful variables that shall be included in the model to produce optimal outcome.

Finally, task 8 including the training of machine learning models and cross validations, allowed establishment of the best performing workflow, for which the results are presented in this report.

Timeline

Tasks	2016				2017								
	Sept.	Oct.	Nov.	Dec.	Jan.	Feb.	Mar.	Apr.	May	June	July	Aug.	Sept.
1. Familiarization with Machine Learnin methodologies													
2. Familiarization with PERL and Yuanfang Guan's approach													
3. Decoding of original scripts													
4. Establishment of baseline implementation													
5. Definition of improvement plan													
6. Re-establishment of training & test set													
7. Feature selection													
8. Cross validation, model optimization & evaluation													
9. Report writing													

Figure 1.1. Plan of work and tasks realized in the project.

2. The AstraZeneca-Sanger Drug Combination Prediction DREAM Challenge

As stated before the goal of this challenge is to expand the understanding of drug synergy and to identify biomarkers driving a patient's response. Although the competition encompasses two subchallenges, the focus of interest was only one of them - closer to the reality, so more interesting and important from this point of view. It reproduces the common situation in personalized medicine where the therapies must be determined and selected only on prior knowledge. Thus, the aim is to predict in vitro drug synergy without the access to the combinational therapy training data. The effect needs to be inferred from multi-sourced molecular data, compound information, experimental results of mono-therapies and/or any relevant prior knowledge and external datasets (Figure 2.1.).

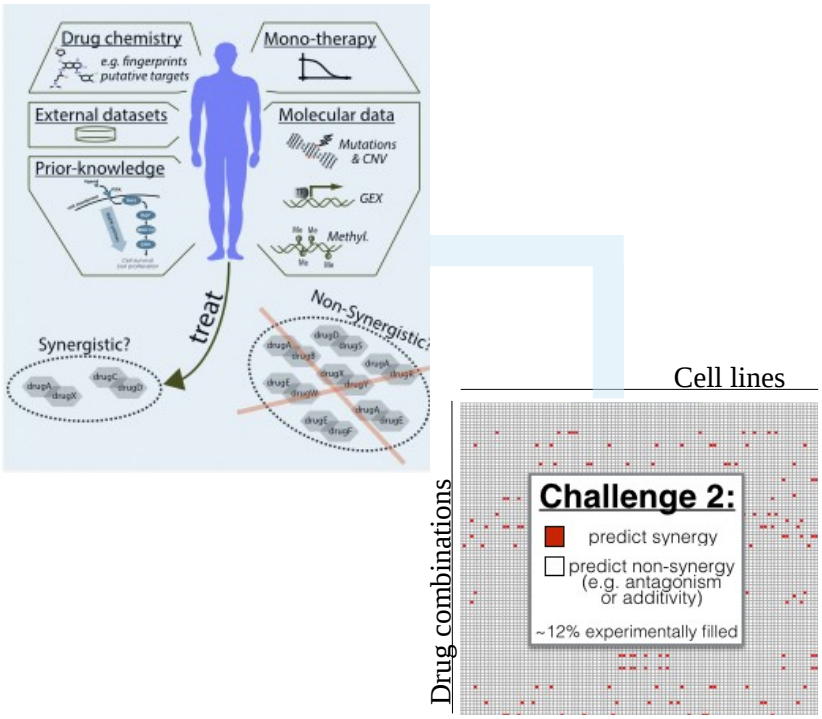

Figure 2.1. Visualization of the concept of subchallenge 2 [19].

Along this work, the gene names and symbols are normalized according to standard defined by the HUGO Gene Nomenclature Committee at the European Bioinformatics Institute. The cell nomenclature is standard and common between worldwide laboratories, uniquely identifying the lines and their origin.

2.1. DREAM Challenge Data

2.1.1. Pharmacological Data

In order to generate the pharmacological data, the experiments on 85 different cancer cell lines belonging to 6 different tissue types (Figure 2.2) were performed. The trials were realized on 910 unique drug-pairs combining 118 unique drugs. If all potential combinations would be considered number of possible observations reaches 586,755, while only ~11.5k (~ 2%) cases were covered in the experimental design. Thus the data space that could be represented in a form of a matrix with axes corresponding to drug 1, drug 2 and the cell line, would be highly sparse turning the modeling even more complex.

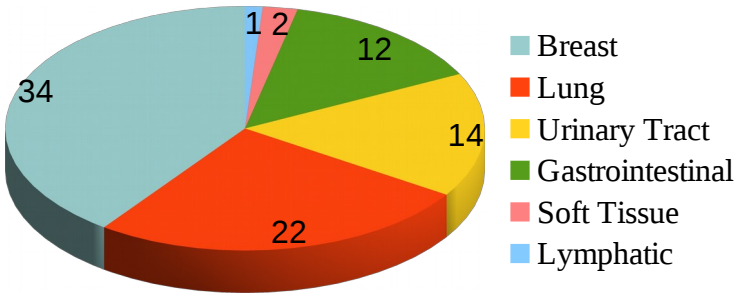

Figure 2.2. Tissue-of-origin of the samples in the study.

The study was constructed on the fundamental concept that any anticancer drug or combination of drugs affects the tumour cells causing their death. This effect is correlated with the dosage of the pharmaceutical applied and can be expressed by the change in the cell viability. Since the very detailed information on assay is needless in the context of this work, only general view on the assay design will be provided, briefly presenting the approach used to estimate such a dose-response curve characterizing the particular cell-treatment process.

On the purpose of the experimental study, the samples were collected giving origin to the cell line cultures that were prepared and afterwards distributed among the plates. Each single tested drug (in case of mono-therapy) or drug-pair (in case of combination therapy) was dosed among the wells with particular cell line in 5 different concentrations per compound. After 5 days of incubation and staining step, the fluorescent intensity was read allowing determination of the numbers of dead cells per each well. Next, the total cell numbers was obtained in re-read of plates and the calculation of the living units was performed. The observed change in living cells (expressed in percentages) was determined due to normalization of computed values to control samples where no treatment was applied.

Mono-therapy

In the mono-therapy assays the single drug is applied to the samples and the response of cancer cells is recorded. Majority of the biological processes follow the sigmoidal form and they are usually summarized by 4-parameter nonlinear logistic equation, the Hill equation [20][21]. The dosage-response curve is fitted to 5 experimental points and in most of the cases approximates to a sigmoidal shape (Figure 2.3.).

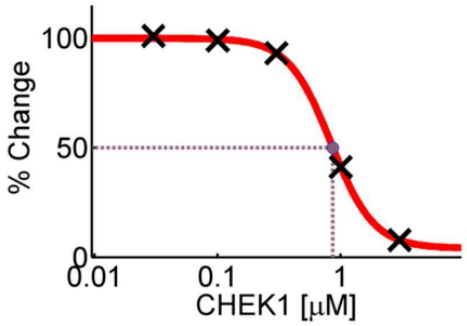

Figure 2.3. Dosage-response curve fitting (Hill equation) for exemplar mono-therapy experiment for CHECK1 drug [22].

As could be expected, the plot reflects a common relation between treatment dosages and cell viability. The low concentrations of drug have null or nearly null effect, leaving 100% of cells alive. Contrary, while applied dose is high, it is able to cause total death of cell culture (0% of survivability). The experimental plots are created by drawing the observed effect E_α against drug concentration α, and they serve for fitting the dosage-respond equation (2.1.).

$$E_\alpha = 100 + \frac{E_\infty - 100}{1 + \left(\frac{IC_{50}}{\alpha}\right)^H} \qquad (2.1.)$$

The determination of coefficients allows characterization of the drug activity in a particular cell through the following parameters: maximum change in cell viability- E_∞, dose causing 50% of maximum cell death- IC_{50} and slope of the plot- H.

Combination therapy

"The search for synergy (...) is reminiscent of Dorothy ["The Wizard of Oz"] and the ruby slippers. (...) it is often assumed that proper and easy synergy assessment is possible but that it is necessary for some wizard to tell us the secret."

Greco et al, 1996 [23]

In the combinatory treatment the effect on a cancer cell survival is observed after application of a two pharmaceuticals simultaneously. In this case the experimental results can be presented in 3-dimensional space where the observed difference in a cell count are plot against the plane of two drug concentrations (Figure 2.4.) creating dosage-response surface.

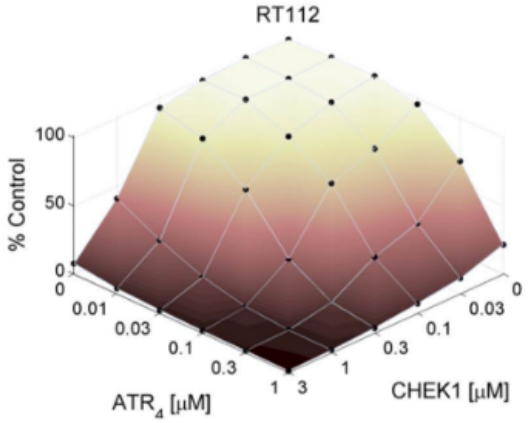

Figure 2.4. Dosage-response surface fitting. Example of combinatory therapy outcome for drug pair ATR_4 and CHEK1, carried out on human bladder carcin.oma RT112 cell line [22].

The dosage-response surface reflecting observed effect (*E*) consists of two sublayers that correspond to additive (*A*) and synergistic (*S*) effects (Figure 2.5.). First of components is understand as a basic response when the combination stays neutral and does not affect the cancer cells in any manner. The extra effect *S* is the one that actually causes the change in cell viability. Thus, it is the aim of interest since it captures the synergistic (if positive) or antagonistic (when negative) character of relation

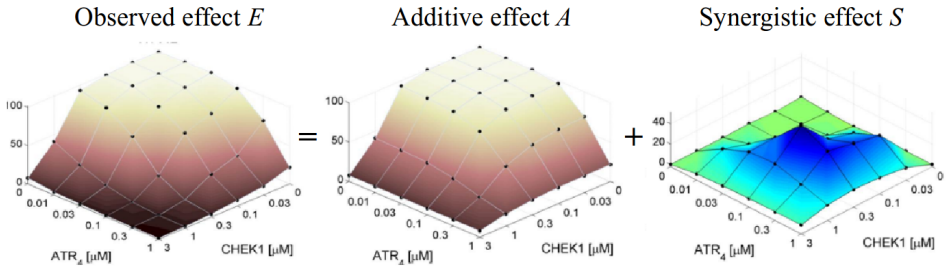

between the two drugs, when acting on a particular cell line.

Figure 2.5. Graphical representation of principle for computation of the extra-effect (S) distribution [22].

In order to estimate the extra effect, the additive effect is determined on mono-therapy data [17] and afterwards subtracted from the observed one. This is accomplished applying the Loewe model [24] [25], which relies on the isobole equation. Firstly, the baseline effect *A* is calculated by solving numerically the referred equation for all dose concentrations and next the synergistic effect layer *S* is derived. In order to express the extra effect by a single value, the distribution of S is integrated in function of logarithmic drug concentrations space, and the total synergy score (*SS*) is delivered.

Data Structure

The Combenefit[1] is an open-source platform providing advanced visualisation tools and model-based quantification and analysis methods for drug combination trials [26]. It was utilized to organize and manipulate the raw experimental outcomes, to fit the Hill equation to data points, to compute the coefficients and calculate the total synergy scores.

For the use of the software, the experimental results are stored in separate standard *.xls* and *.csv* files for each drug pair – cell line combination, created according to the specifications. The template is equal for mono- and combinatory therapies (Figure 2.6.). The top part records the cell counts obtained for all dose concentrations for both compounds. In the bottom, specification of run experiment can be found- identification of drug combination, the name of cell line and units used to express the concentration.

[1] http://sourceforge.net/projects/combenefit/; Last accessed on 17/09/2017

	0,00	Dose 1	Dose 2	Dose 3	Dose 4	Dose 5	(=Agent 2)
0,00	100,00	Data	Data	Data	Data	Data	
Dose 1	Data	Data	Data	Data	Data	Data	
Dose 2	Data	Data	Data	Data	Data	Data	
Dose 3	Data	Data	Data	Data	Data	Data	
Dose 4	Data	Data	Data	Data	Data	Data	
Dose 5	Data	Data	Data	Data	Data	Data	
(=Agent 1)							
Agent 1	Drug A name						
Agent 2	Drug B name						
Unit1	Concentration (\muM)						
Unit2	Concentration (\muM)						
Title	Cell line name						

Figure 2.6. Structure of the *.xls* and *.csv* files storing information on combination and mono-therapy assays.
* 'Data' - Numeric; Percentage of survivor tumour cells observed for each treatment.
* 'Data' - as above; available only for combination therapy assays.

Some of the trials had to be repeated due to unsatisfactory level of quality of the measurements and all the experiments are recorded in separate files. The duplicates and triplicates are identified by the adequate suffix in the file name, respectively: **.Rep2* and **.Rep3*. In total there are 11,759 available files corresponding to the mono-therapy assays and 6,731 storing the results of combinatory experiments.

After Combenefit manipulations, plotting and Hill's equation fitting, the results are summarized and stored in a *.csv* file with 14 fields (Appendix 1A). Among the recorded information, there can be found combinatory effect coefficients, quality assessment, specification of a drug pair – cell line combination and finally the total synergy score value.

2.1.2. Molecular Data

Three molecular data sources: gene expression, copy number variants and mutations in cancer cell lines, were produced in a frame of one of the Sanger Institute projects, namely the Genomics of Drug Sensitivity in Cancer (GDSC). The methylation data was generated by the Estseller group from Bellvitge Biomedical Research Institute (IDIBELL). All this molecular data provided within the DREAM challenge is available at COSMIC repository (COSMIC2012) in a format of *.csv* files. The gene names and symbols used in the work are normalized according to standard defined by the HUGO Gene Nomenclature Committee at the European Bioinformatics Institute. To allow easy transfer and sharing of information, the cell nomenclature is standard and common among worldwide laboratories, uniquely identifying the lines and their origin.

Gene Expression

Regarding to the data on RNA expression, it comes from a study performed using Affymetrix Human Genome U219 Array Plates, available at ArrayExpress platform: E-MTAB-3610 [27]. The values provided was obtained after processing the raw data in R utilizing tools implemented within the Bioconductor [28]. Firstly, the package '*makecdfenv*' [29] was applied to read Affymetrix chip description file (CDF) and allow mapping between probes and genes. Next, the values were normalized with Robust Multi-array Average (RMA) algorithm employing R-package '*affy*' [30]. The 2-dimensional matrix holding processed values of a gene expression has 83 rows listing the cell lines and 17,419 columns corresponding to the genes. It also contains missing values due to the unavailable data for two cell lines: MDA-MB-175-VII and NCI-H1437.

Copy Number Variations

Another data set provides the knowledge on Copy Number Variations (CNVs). It was generated employing Affymetrix SNP6.0 microarrays and can be found at European Genome-phenome Archive: EGAS00001000978 [27]. The chromosomal alterations were identified using the *PICNIC* algorithm [31] with the reference to 38 human genome build (GRCh38). The data provided reveals the state of chromosome at two levels: of the segment and gene. Since the approach presented in this work focuses on genes and simulates the posterior state on the gene level, exclusively the last source of CNV information was considered in the preparation of the model. The respective *.csv* file is a list of CNVs that encompasses 29,158 observations for each of 85 cell lines (that is 2 478,430 unique records in total) and contains 9 fields (Appendix 1B) revealing specifications of each gene alteration.

Mutations

In order to obtain detailed mutational profile for the cancer cell lines, the whole exome sequencing was performed with the Agilent's SureSelect on the Ilumina HiSeq 2000 platform. Raw BAM files are available on repository with mentioned above CNV data (EGAS00001000978 [27]). Two algorithms were applied to identify mutations, namely the CaVEMan (Cancer Variants Through Expectation Maximization) and PINDEL [32], allowing calling of the total 75,281 mutations for all 85 cell lines. The resulted output data was organized in a single *.csv* file with 32 fields (Aappendix 1C) including all the specifications and details of detected mutation.

Methylation

One of a studies held at IDIBELL Institute and carried by the Esteller team provided the molecular data on methylation. The project was performed at Illumina Infinium HumanMethylation450 v1.2 BeadChip platform and the raw data is stored at a public Gene Expression Omnibus **(**GEO) repository: GSE68379 [27]. The methylation status can be expressed by two different parameters [33]:

- the $beta_i$ methylation status of y_i CpG site, which is a ratio of maximal methylated probe intensity versus the total sum of maximum methylated and unmethylated intensities (Eq. 2.2.);

$$beta_i = \frac{max(y_{i,methylated}, 0)}{max(y_{i,methylated}, 0) + max(y_{i,unmethylated}, 0) + \alpha} \qquad (2.2.)$$

- value M_i, expressed as logarithm of ratio of maximum methylated and unmethylated probe intensities (Eq. 2.3.).

$$M_i = \log_2\left(\frac{max(y_{i,methylated}, 0) + \alpha}{max(y_{i,unmethylated}, 0) + \alpha}\right) \qquad (2.3.)$$

Both metrics are computed with correction through a coefficient α that is variable specific for the platform used in the assay, in this case – one recommended for Illumina. Available *beta* and *M* scores are defined per probe and CpG island. Thus, there are four datasets provided with methylation status expressed by *beta* and *M* metrics, probe- and island- wisely each. Following Yuanfang Guan, unlogged ratios assigned per probe were used as involving less transformations on raw values. The methylation data is organized within the 2-dimensional matrix with 28,7450 rows referring to all unique probes included in the assay and 82 columns corresponding to the studied cell lines (unavailable data for MDA-MB-175-VII, KMS-11, SW620).

2.1.3. Compound Data

The data on chemical and structural properties for 118 unique drugs involved in the experiments is provided in the *.txt* file with 8 fields (Appendix 1D). For each compound with anonymised name, chemical and structural properties are specified including the targets of action, specification on H-bond acceptors and donors (HBA and HBD), octanol-water partition coefficient (cLogP), number of fulfilled Lipinski rules (Lipinski), SMILES or PubChem identificaton and molecular weight. Worth of noting is a fact that since the identity of all compounds is anonymized due to a confidentiality agreements, the information on drugs provided within this file is the one to rely on. The only possible alternative to make a connection with a prior knowledge is throught the SMILE or PubChem ID, however this field is unavailable for 33% of instances.

2.2. Submission Form

After building a model, the final predictions could be submitted on a Synapse platform. The accepted format is a comma separated text file holding a synergy prediction matrix that contains cell lines in columns and drug combinations in rows (Figure 2.7.). The predictions shall be expressed in binary form, identifying synergy (=1) and non-synergy (=0). The prediction assigning '0' value to a drug pair – cell line combination, stands for the antagonism, null effect or additivity. The models are tested for ability to determine synergistic instances.

	cell_1	cell_2	cell_3	cell_4	...	cell_85
drugA.drugB	0	1	0	0	...	0
drugA.drugC	0	0	0	0	...	0
drugA.drugD	0	0	1	0	...	1
drugA.drugE	0	0	1	0	...	0
drugA.drugF	0	0	0	0	...	0
drugA.drugG	0	0	0	1	...	0
...	...	...	...	...	...	...
drugX.drugY	0	0	0	0	...	0

Figure 2.7. Form of synergy prediction matrix accepted for final submission in subchallenge 2 [34].

The participants were also asked to provide the *.csv* file, equally structured, containing confidence scores of corresponding produced predictions. However, it is not relevant in the context of this work and so its description is omitted.

3. The Winning Solution

"Always try the easiest solution.
And the common sense – first."
Y. Guan

This work was inspired on the winning solution of the 2016 AstraZeneca-Sanger Drug Combination Prediction DREAM Challenge. The implementation is provided by exceptional researcher Yuanfang Guan from a Department of Computational Medicine and Bioinformatics at University of Michigan. Over last 4 years she with her team participated in 7 individual DREAM competitions, some consisting of 2 or 3 subchallenges, always being recognized among the top performing teams. Fifteen submissions of GuanLab became 1st place winning solutions (Table 3.1.), including challenges on various diseases (ex. cancers, Alzheimer, Rheumatoid Arthritis) and broad range of tasks to solve (classification, prediction, inferrence problems). This achievements prove the excelence and efficiency of the built models. There is no doubt that general approach of problem solving developed by Guan deserves an attention and is a valuable lesson to learn.

Although each of submmissions is provided with script files and supporting documentation, usually the given explanations are not sufficient to easily understand and accurately reproduce the methodology. Exploration of Guan's implementation requires careful examination and backtracking of scripts, with simultaneous connecting it to the interpretation. Task become even more complicated due to:

- absence of dockstrings and comments in scripts;

- unclean script writting, with remains of experimented commands;

- redundant programming - unnecessary manipulations, ghost-variables;

- presence of unutilized scripts – files are submitted but never called and run by wrapping script;

- unclear origin of some input files;

- unknown pre-processing of original files.

Untill now some manipulations remain ambiguous but it was pretended to follow the indication of the proper author cited in the opening of this chapter. The effort was made to create a reconstruction of procedure as close to the original as possible.

The workflow of the baseline implementation include four main steps:

1) Building of feature vectors;

2) Generation of models;

3) Merging of predictions;

4) Identification of synergy.

Yuanfang Guan extended a model by including additional information as presented in the following section 3.1. Outsourced Data.

Table 3.1. GuanLab's 1st place submissions to DREAM Challenge [35].

Year	**Challenge**	**Problem/Data**
2017	ENCODE-DREAM in vivo Transcription Factor Binding Site Prediction Challenge	Predicting Transcription Factor Binding Sites
2016	ICGC-TCGA-DREAM Somatic Mutation Calling Challenge -- Tumor Heterogeneity and Evolution	Inferring tumor heterogeneity and subclone reconstruction
2016	AstraZeneca-Sanger Drug Combination Prediction DREAM Challenge	1a. Predict drug synergy using drug combinational training data, expression, CNV, mutation, drug chemical space
2016	AstraZeneca-Sanger Drug Combination Prediction DREAM Challenge	1b. Predict drug synergy using CNV, mutation and drug chemical space
2016	AstraZeneca-Sanger Drug Combination Prediction DREAM Challenge	2. Predict drug synergy without drug combinational training data (unseen drug pairs)
2015	ALS Stratification Prize4Life Challenge	1. Predict survival in ALS PROACT data
2015	ALS Stratification Prize4Life Challenge	3. Predict survival for national registry data
2015	Olfaction Challenge	1. Predict olfaction response for individuals using chemical structure data
2015	Prostate Cancer Challenge	2. Predict which patients cannot tolerate chemotherapy
2014	Rheumatoid Arthritis Challenge	1. Predict patient response to different drugs
2014	Rheumatoid Arthritis Challenge	2. Predict non-responders
2014	Alzheimer BigData Challenge #1	1. Predict the prognosis of AD patients
2014	Alzheimer BigData Challenge #1	3. Classify individuals into diagnostic groups using MR imaging
2014	Broad Institute Gene Essentiality Challenge	2. Identify the most predictive biomarkers to predict cancer cell survivability under small molecule perturbations
2013	Breast Cancer Network Inference	2. Drug response of phosphorylation network prediction in cancer cells

3.1. Outsourced Data

Beside the DREAM challenge data, Guan's implementation introduced the additional prior knowledge including molecular and functional network information. The data on RNA expression and Copy Number Variants was outsourced from The Cancer Cell Line Encyclopedia (CCLE2012)[2]. This project is a successful result of a partnership between the Broad Institute, and the Novartis Institutes for Biomedical Research and its Genomics Institute of the Novartis Research Foundation [36]. Althought the data is available for more than 1,000 of cancer cells, requiring the filtering of information for relative DREAM samples, for both sources there are missing measurements for M14, MFM-223 and NCI-H3122 lines.

Regarding the functional network data source, Yuanfang Guan included a prediction FNTM server for tissue-specific protein interactions for the laboratory mouse *Mus musculus* which the most widely used model organism for human disease [37].

3.1.1. CCLE Expression

The outsourced gene expression data comes from a study performed using Affymetrix GeneChip Human Genome U133 Plus 2.0 platform. The raw values provided with *.CEL* files were merged and summarized for each probe set with Robust Multi-array Average (RMA) algorithm. The quantile normalization was applied in order to remove the array-specific effects and guarantee the identical statical properties of different measurement distributions among the trials. The annotation of genes was accomplished according to the custom *.CDF* file released on 18th of January 2012 (ENTREZG, version 15). The dataset is a 2-dimensional matrix with 18,988 probes with assigned genes (if applicable) and total of 1,037 human tumour cell lines.

3.1.2. CCLE CNVs

Another prior knowledge was provided within the study carried on Affymetrix Genome-Wide Human SNP Array 6.0., bringing the additional molecular information on CNVs. After merging the *.CEL* files, linear calibration curves were estimated for each probe set, allowing identification of the copy numbers.The measurements were normalized utilizing the most similar HapMap control sample as reference. The circular binary segmentation (CBS) algorithm was applied in order to call segments on log2 ratios. Obtained dataset has a structure of 2-dimensional matrix with the copy number values for 23,316 genes and 1,043 cell lines.

3.1.3. Functional Networks of Tissues in Mouse

The functional network predicts the probability that a pair of proteins is involved in the same biological process. One of the most comprehensive platforms holding this data - Functional Networks of Tissues in Mouse (FNTM) [37], was created by Laboratory for Bioinformatics and Functional Genomics in the Lewis-Sigler Institute for Integrative Genomics at Princeton University, and is free available[3]. It was a database of preference since Yuanfang Guan is probably highly familiar and closely connected with the work, considering a fact that her PhD in Molecular Biology, as well as Postdoctoral Fellow in Integrative Genomics were both accomplished at Princeton University.

[2] https://portals.broadinstitute.org/ccle; Last accessed on 21/09/2017

[3] http://fntm.princeton.edu/; Last accessed on 22/09/2017

In order to generate the network in mouse, diverse data sources needed to be integrated: gene expression, tissue localization, phylogenetic and phenotypic profiles, data based on homology, physical interactions and gene-disease/phenotypic associations. According to the Yuanfang Guan [38] creating such a functional network in mammalian models is still challenging. Thus using the much simpler mouse network that could reveal major connections and relations between proteins could be applicable in human models by inference.

In brief, according to the author, the procedure of determining the functional relations between the genes and their connection probabilities encompasses five main steps [39]:

1) Pick all possible files with available data related to genes, for example microarrays, RNA-seq, phenotypes, sequences, homologies etc.

2) Compute correlations between genes and normalize them using z-transform.

3) Build a gold standard set using KEGG/GO.

4) Bin each into a number of bins.

5) Compute the Bayesian posterior with some regularization.

As could be expected this process is computationally highly intensive.

3.2. Feature Vectors

The final predictions are obtained by computing a weighted average from six separate models:

- global molecular,
- global mono-therapy,
- chemical,
- file-counting,
- local molecular,
- and local mono-therapy.

Each of those involves independent construction of feature vectors, for which different data sets serve as a sources and particular handling and manipulation steps are implicated.

3.2.1. Global Molecular

The molecular feature vector is based on six *i* data sources: gene expression, CNVs, mutations and methylation that are described in details in the section 2.1.2., and additional outsourced CCLE data presented in sections 3.1.1. and 3.1.2. The files selected to be used characterize a molecular profile of cancer samples with regard to collection of genes. Each of them is transformed into unifrom two-dimensional matrix (Figure 3.1.) where the columns refers to the cell lines and rows- to genes. They are filled with $v_{G1} - v_{Gn}$ values corresponding to an exact cell - gene instance, and expressing the assay results provided with each original data source. Thus, in case of quantitative measurements, RNA expression and methylation, they remain represented by respectively: logged intensities and level of methylation (ranging from 0 to 1 that corresponds to 0% – 100% of methylation). For qualitative properties like CNVs and mutations, those must be binarized assigning value '1' when the alteration is present and '0' contrary. All those matrices serve as input for the baseline script.

Worth noting is a fact that the exact files, as well as a procedure of file preparation and matrix construction is not revealed by the author, this knowledge was inferred from posterior manipulation steps written in PERL. However still remains unclear what approach was applied regard to missing values.

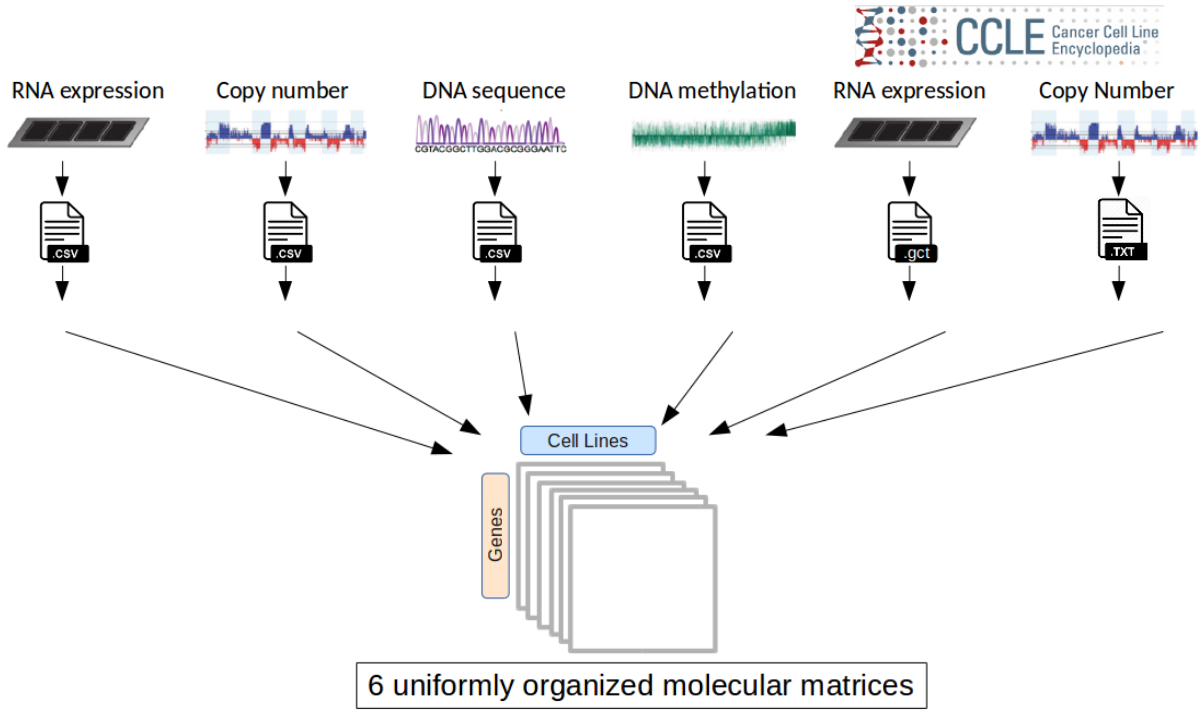

Figure 3.1. Visualization of the pre-processing step applied to six molecular data sources according to baseline implementation.

The construction of Global Molecular Feature Vector, $FV_{GlobalMolecular}$, encompasses three main steps:

1. Building of prior feature vectors, fv_i, corresponding to individual data sources;
2. Simulation of molecular data under the drug;
3. Composition of posterior $FV_{GlobalMolecular.}$

Prior feature vectors

Each of six uniform matrices serves for construction of a proper dictionary holding the set of partial feature vectors fv_i, as values assigned to unique $[CL]$ cell line keys (Eq. 3.1.). The sequence of variables in each of vectors follows determined order of genes $G_1 - G_n$. Yuanfang Guan limited the features included in construction of vectors exclusively to a set of target genes (Figure 3.2.).

$$fv_i[CL] = [v_{G1,}, v_{G2,}, v_{G3,} \dots, v_{Gn}] \quad (3.1)$$

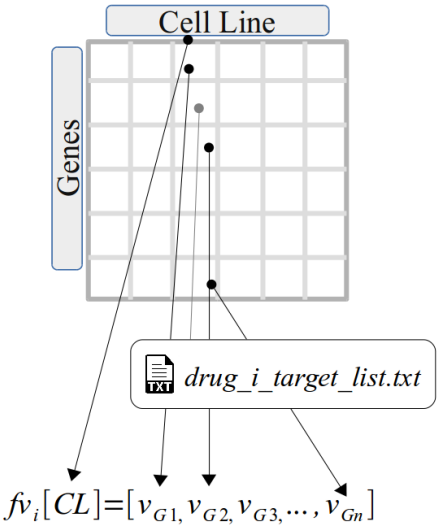

Figure 3.2. Visualization of construction of partial feature vectors fv_i, from uniform matrices holding molecular data, with a step of filtering target genes.

All molecular sets have their particular target gene lists. Those were apparently created from the challenge data file on chemical and structural properties of drugs (2.1.3. Compound Data), with regard to genetic property. Again, the process of preparation is unrecorded, however the specific gene lists used in the implementation were generously provided by the author after the final submission.

As a result, six dictionaries are created holding prior feature vectors: fv_{exp}, fv_{cnv}, fv_{mut}, fv_{meth}, $fv_{CCLEexp}$, $fv_{CCLEcnv}$, corresponding to cancer cell lines, and based on respective data source: RNA expression, CNVs, mutations, methylation, CCLE expression and CCLE CNVs.

Simulation of molecular data under the drug

Importantly, this is a key step. Molecular data provided in the challenge (see details in section 2.1.2. Molecular Data) is basically useless if not simulated to posterior values under the applied drugs. In order to obtain the molecular profiles after the treatment for each cell line – drug pair case, the prior knowledge from FNTM (see 3.1.3. Functional Networks of Tissues in Mouse) was used. The principal idea was to alter each original state according to the probability of connection between two genes: the target gene for the particular drug and the gene in consideration. The simulation was performed basing on the source *.txt* file provided by the Yuanfang Guan beside the submitted solution. The file contains information on the architecture of the functional network in the mouse. Thus, each line corresponding to a single connection indicates two genes and the value of linkage probability (Figure 3.3.), including in total the network of 211778490 relations.

```
head guan_bayesnet_integration.txt
MGI:88313       MGI:88357       0.999992
MGI:97380       MGI:97384       0.999986
MGI:97848       MGI:97849       0.999983
MGI:104772      MGI:88313       0.999977
MGI:95574       MGI:96646       0.999976
MGI:96952       MGI:98834       0.999974
MGI:101816      MGI:101938      0.999972
MGI:107674      MGI:88127       0.999963
MGI:88302       MGI:88351       0.999961
MGI:103290      MGI:97312       0.99996
```

Figure 3.3. Inspection of the head of source file containing information on probability of connections in functional network in mouse.

As could be expected, the names of genes are expressed according to the official nomenclature established by the International Comitee on Standardized Genetic Nomenclature for Mice that is available in the Mouse Genome Informatics Database[4]. In order to take advantage of this information, the MGI identificators require to be converted to HGNC nomenclature used as a standard. The file called by PERL script in order to accomplish the translation was not originally provided. It was found throught the search in the internet and downloaded from the GitHub repository[5], thank to the *nkiip* user that generously shared a file on the 15th of May 2016 and made it available.

The concept of simulation follows the common sense and reflect the simplified reality. The basic assumptions are:

1) The efficiency of treatments is ideal and once applied they totally turn off the genes that are the drug targets.

2) The genes that are not targets for applied drug, neither connected to target genes: their state remains unchanged (the treatment has no effect on them).

3) Treatment alterates the state of genes related to the drug targets according to the connection probability between those genes.

For the special attention deserves last of the rules. It cannot be applied automatically since the 'direction' of alteration must be considered, i.e. if the molecular state promotes or limits the carcinogenesis. The action of a drug is always directional: contra the tumour, what means that it shall promote anticancer events and reduce those which are pro. Following the general rules stated above, particular cases can be considered.

Concerning expression, the gene state for each cell line is described by the *log2* of measured intensity so the matrix is filled with continuous values. The expression of the gene that is a drug target for the applied drug turns zero- reflecting the total silencing. Genes that are functionally linked to the target reduce their intensities according to the connection probability (Eq. 3.2.). This simulation approach is valid for both expression data sources – one provided within the challenge and other outsourced from the CCLE platform.

$$v_{Gn}[\exp, posterior] = v_{Gn}[\exp, prior] * (1 - p_{connection}) \qquad (3.2.)$$

The information in a CNV matrix is binarized, expressing the gene states by discrete data. According to the main concept, target genes turn zero because their activity is totally recovered under a treatment, and the copy number does not promote the growth of cancer any more. The activity of connected genes becomes partially normalized, their status reduces proportionally to the linkage with a target, and in consequence has less impact on tumorigenesis (Eq. 3.3.). The simulation of a CNVs posterior status for a dataset outsourced from CCLE shares the same logic.

$$v_{Gn}[cnv, posterior] = v_{Gn}[cnv, prior] * (1 - p_{connection}) \qquad (3.3.)$$

For mutations that are also organized in binary matrix, the assumption of ideal treatment would be high to far unrealistic. This is an exception since the drugs applied nowadays are yet unable to fix the pro-cancer mutations in any manner. Thus, the state of target genes remains unchanged while values assigned to related genes are multiplied by the connection probability (Eq. 3.4.). Note, that in this case the manipulation will always bring reduction of a molecular state: gene carrying mutation is assigned with '1' and if is connected to target, will turn < 1, according to a probability that is always below 1. It can be interpreted as although the target mutation cannot be fixed, the treatment will have still an indirect impact, improving other related processes.

$$v_{Gn}[mut, posterior] = v_{Gn}[mut, prior] * (1 - p_{connection}) \qquad (3.4.)$$

[4] http://www.informatics.jax.org/mgihome/nomen/; Last accessed on 22/09/2017;

[5] https://github.com/nkiip/GC2NMF/blob/master/0_origin_data/MGI_Gene.rpt; Last accessed on 25/09/2017;

In the case of methylation, matrix is filled with continues values that range between 0 and 1 and that correspond to a percentage of methylation level. The simulation according to Yuanfang Guan is practically proceeded as follows: the target genes become totally unmethylated while the related genes proportionally decrease their methylation level. However the script does not correspond to the documentation [39]. The author states that for both- target genes and those connected, status turns bigger (proportionally to the connection probability in latter case, as usually).

Due to this discrepancy, the additional research was performed to understand the methylation processes underlying the carcinoma and decide on approach to implement. In cancer cell lines two phenomena are observed [40][41]:

- hypermethylation of CpG sites that causes the inactivation of tumor-suppressor genes,

- genome widespread hypomethylation that promotes the carcinogenesis and the tumor progression.

Remembering that the data provided in challenge contains the measurements captured in CpG sites, it seems reasonable and convincing to define the process of simulation under the drug as followes: the target genes become totally unmethylated turning their status to zero (allowing tumor-suppressor genes to fight against the cancer), while related genes reduce the methylation level according to the connection probability (Eq. 3.5.). This approach, equal to included in PERL script, was proved to result in more accurate model and so was decided to be implemented in this work.

$$v_{Gn}[met, posterior] = v_{Gn}[met, prior] * (1 - p_{connection}) \quad (3.5.)$$

Interestingly, Yuanfang Guan claims that the inclusion of methylation data apparently hurts the performance [39]. This fact confirms the theory that proposed methodology of methyl simulation could be imperfect and an alternative manner shall be applied.

Summarizing, each of prior feature vectors is processed and all $v_{G1} - v_{Gn}$ values are substituted with a new state, generating simulated feture vectors, fv'_i.

Posterior feature vectors

In order to generate the global molecular feature vectors $FV_{GlobalMolecular}$, reflecting the molecular profiles of samples, the simulated partial feature vectors are joined (Eq. 3.6.) according to their cell line annotation.

$$FV_{GlobalMolecular}[CL] = [fv'_{\exp}, fv'_{cnv}, fv'_{mut}, fv'_{met}, fv'_{CCLEexp}, fv'_{CCLEcnv}] \quad (3.6.)$$

3.2.2. Global Mono-therapy

The idea of mono-therapy modeling is to produce the predictions basing on pharmacological sources with the experimental and curve-fitted variables. The feature vector is constructed from the original cell counts observed in assays and estimated Hill model parameters. Due to a complexity of the procedure it is convenient to define some common terminology for the purpose of this work, to provide clearer and simpler description of the data manipulation.

Along this lines, denomination '$y_{A1\text{-}5}$' is used for cell counts obtained under the drug *A* for five different dosages. Similarly, '$y_{B1\text{-}5}$' stands for changes in cell viability observed for five concentrations of drug *B*. Recalling the coefficients estimated by curve-fitting, the following designation of variables is applied:

MAX_CONC_A → z_{A1}
MAX_CONC_B → z_{B1}
IC_50_A → z_{A2}
IC_50_B → z_{A2}
H_A → z_{A3}
H_B → z_{A3}
Einf_A → z_{A4}
Einf_B → z_{A4}

The construction of global mono-therapy feature vector $FV_{GlobalMonotherapy}$, encompasses six basic steps that are repeated for three different ways of ordering variables identified as: 'max_min', 'B_A' and 'A_B'. Thus, in total there are 18 partial feature vectors (6 x 3 orders) that are created by the same number of separate PERL scripts and saved in individual *.txt* files. Unlike in the case of a global molecular feature vector, which was generated for each cancer sample, here it is required to build a vector for each drug pair - cell line combination [*drugA.drugB.CL*]. Equations pesented below (3.7. - 3.18.) express the algorithms applied in order to generate the partial feature vectors fv_i, where index '*exp*' indicates a vector based on experimental data, i.e. the cell counts, and '*eqHill*' - on parameters computed in dosage-response curve fitting.

$$fv_{exp,max\_min}[drugA.drugB.CL] = \left(max(y_{A1},y_{B1}), min(y_{A1},y_{B1}), (y_{A1}+y_{B1}), \ldots, max(y_{Ai},y_{Bi}), min(y_{Ai},y_{Bi}), (y_{Ai}+y_{Bi})\right) \quad (3.7.)$$

$$fv'_{exp,\,max\_min}[drugA.drugB.CL] = fv_{exp,\,max\_min}[drugA.drugB.CL] - \frac{\left(avg(y_{drugA.CL.i}) + avg(y_{drugB.CL.i})\right)}{2} \quad (3.8.)$$

$$fv''_{exp,max\_min}[drugA.drugB.CL] = fv_{exp,\,max\_min}[drugA.drugB.CL] - avg(y_{CL.i}) \quad (3.9.)$$

$$fv_{eqHill,\,max\_min}[drugA.drugB.CL] = \left(max(z_{A1\text{-}2}, z_{B1\text{-}2}), min(z_{A1\text{-}2}, z_{B1\text{-}2}), \log(z_{A1\text{-}2} + z_{B1\text{-}2}), \ldots, max(z_{A3\text{-}4}, z_{B3\text{-}4}), min(z_{A3\text{-}4}, z_{B3\text{-}4}), (z_{A3\text{-}4} + z_{B3\text{-}4})\right) \quad (3.10.)$$

$$fv'_{eqHill,\,max\_min}[drugA.drugB.CL] = fv_{eqHill,\,max\_min}[drugA.drugB.CL] - \frac{\left(avg(z_{drugA.CL.i}) + avg(z_{drugB.CL.i})\right)}{2} \quad (3.11.)$$

$$fv''_{eqHill,\,max\_min}[drugA.drugB.CL] = fv_{eqHill,\,max\_min}[drugA.drugB.CL] - avg(z_{CL.i}) \quad (3.12.)$$

$$fv_{exp}[drugA.drugB.CL] = (y_{B1\text{-}5}, y_{A1\text{-}5}) \quad (3.13.)$$

$$fv'_{exp,B\_A}[drugA.drugB.CL] = \left(fv_{exp,\,B\_A}[drugA.drugB.CL]_{1\text{-}5} - avg(y_{drugB.CL.i}), fv_{exp,\,B\_A}[drugA.drugB.CL]_{6\text{-}10} - avg(y_{drugA.CL.i})\right) \quad (3.14.)$$

$$fv''_{exp}[drugA.drugB.CL] = fv_{exp}[drugA.drugB.CL] - avg(y_{CL.i}) \quad (3.15.)$$

$$fv_{eqHill,\,B\_A}[drugA.drugB.CL] = \left(z_{A1}, z_{B1}, \log(z_{A1} + z_{B1}), z_{A2}, z_{B2}, \log(z_{A2} + z_{B2}), z_{A3}, z_{B3}, (z_{A3} + z_{B3}), z_{A4}, z_{B4}, (z_{A4} + z_{B4})\right) \quad (3.16.)$$

$$fv'_{eqHill,\ B\_A}[drugA.drugB.CL] = \left(fv_{eqHill,\ B\_A}[drugA.drugB.CL]_{1,3,4,5} - avg\left(z_{drugA.CL.i}\right),\ \mathrm{fv}_{eqHill,\ B\_A}[drugA.drugB.CL]_{2,6,7,8} - avg\left(z_{drugB.CL.i}\right)\right) \quad (3.17.)$$

$$fv''_{eqHill,\ B\_A}[drugA.drugB.CL] = fv_{eqHill,\ B\_A}[drugA.drugB.CL] - avg\left(z_{CL.i}\right) \quad (3.18.)$$

The process of generation of resting six partial feature vectors fv_i, corresponding to 'A_B' ordering is analogous to approach expressed by equations 3.13. – 3.18., just with a reversed sequence of variables.

Finally, the global mono-therapy feature vectors are generated by merging of all the produced partial vectors (Eq. 3.19.) regarding to a specific drug pair - cell line combination [drugA.drugB.CL] correspondence. Thus each of them includes 189 predictor variables.

$$FV_{GlobalMonotherapy}[drugA.drugB.CL] = [fv_{exp,\ max\_min},\ fv'_{exp,\ max\_min},\ fv''_{exp,\ max\_min},\ fv_{eqHill,\ max\_min},\ fv'_{eqHill,\ max\_min},\ fv''_{eqHill,\ max\_min}, \ldots] \quad (3.19.)$$

3.2.3. Chemical

One of the simplest and quickest to generate is the chemical feature vector, $FV_{Chemical}$. The file holding information on specific properties of drugs (see 2.1.3. Compound Data) contains large amount of missing data: among 119 observations only 58 contain complete information. It is totally unclear how Yuanfang Guan decided to deal with this issue since the direct input file entering the PERL script is not provided, neither described by the author.

For each drug pair - cell line combination [*drugA.drugB.CL*], two chemical feature vectors are created. The difference between them is again in the order of variables. Thus one of the vectors consider the '*A_B*' order while another – reverse. They encompass five variables, characterizing each of drugs from applied pair (resulting in 10 in total), namely: number of H-bond acceptors and donors (*HBA* and *HBD*), calculated octanol-water partition coefficient (*cLogP*), the number of fulfilled Lipinski rules (*Lipinski*) and molecular weight (*MW*) (Eq. 3.20. and Eq. 3.21.).

$$FV_{Chemical}[drugA.drugB.CL] = [HBA_A, cLogP'_A, HBD_A, Lipinski_A, MW_A, HBA_B, cLogP_B, HBD_B, Lipinski_B, MW_B] \quad (3.20.)$$

$$FV'_{Chemical}[drugA.drugB.CL] = [HBA_B, cLogP'_B, HBD_B, Lipinski_B, MW_B, HBA_A, cLogP_A, HBD_A, Lipinski_A, MW_A] \quad (3.21.)$$

Since the prediction for each combination is doubled and based on original and reversed order of drugs, the model become immune for the fact which of compounds in a pair is indicated as a first, and which as a second.

3.2.4. File-counting

Putting it simple, the idea of file-counting branch is to build a model basing on the amount of information available. That is important since the experiments were not equally performed - the number of assays carried on cancer samples differ among the cell lines (for some there are more data available than for others). Also the drugs were not uniformly included in run tests and in the effect the knowledge on their action is not identical. In order to generate a fair final model this imbalance is taken into consideration.

No pre-processing is required in file-counting branch and the feature vector can be created straightforwardly. The PERL script run through all the experimental files that are available saving and analysing their names. Since the denomination of files follows common pattern: *drugA.drugB.CL.Rep[0-9].csv* it is enough to extract the necessary information on drug pair and cell line used in assay. Passing all the names, the total counts of interest are produced:

- number of files corresponding to a particular cell line: *# files[CL]*,

- number of files corresponding to a particular drug: *# files[drugA] and # files[drugB]*,

- and number of files corresponding to a particular pair of cell and drug (considering drugA and drugB separately): *# files[drugA.CL]* and *# files[drugB.CL]*.

Finally, for each drug pair - cell line combination, two file-counting feature vectors are created (Eq. 3.22. and Eq. 3.23.). They encompass five variables: three are the direct counts obtained as described

$$FV_{[drugA.drugB.CL]} = \left(\#files[CL], \#files[drugA], \#files[drugA.CL], \frac{\#files[drugA.CL]}{\#files[drugA]}, \frac{\#files[drugA.CL]}{\#files[CL]}\right) \quad (3.23.)$$

$$FV_{File\text{-}counting}[drugA.drugB.CL] = \left(\#files[CL], \#files[drugB], \#files[drugB.CL], \frac{\#files[drugB.CL]}{\#files[drugB]}, \frac{\#files[drugB.CL]}{\#files[CL]}\right) \quad (3.24.)$$

above and additional two are the ratios created on base of direct counts.

Contrary to previously presented doubled feature vectors for chemical data, those two do not enter together to the model building step. Separate predictions are produced basing on the information corresponding to the *drugA* and to the *drugB*, and averaged only afterwards giving the final output.

3.2.5. Local Molecular and Mono-therapy

Those two feature vectors are created as their global versions already described (see 3.2.1. Global Molecular and 3.2.2. Global Mono-therapy). The difference comes afterwards, only while building the models. Due to this fact, more details on this mattter can be found in the following section.

3.3. Models

Following the approach of Yuanfang Guan, the random forest algorithm is applied to built the predictive models. Original PERL scripts call the *TreeBagger()* function implemented in the MathLab [42]. The separate models are created for each future vectors, growing 200 trees for each, using all variables as the sets of predictors. The response or outcome variable is the total synergy score, drug pair – normalized. The predictions obtained from each partial model, are saved in individual *.txt* files with a standard structure, where each line contains identification of a cell line, drug pair combination and the predicted value (Figure 3.4.).

```
head pred_ori_0.txt
CELL_LINE,COMBINATION_ID,PREDICTION
HCC1500,CHK1.MTOR_1,18.0308374627
UACC-812,CHK1.MTOR_1,4.67280677142
CAMA-1,CHK1.MTOR_1,35.7371107097
BT-474,CHK1.MTOR_1,8.6866594766
MCF7,CHK1.MTOR_1,14.9264908813
T47D,CHK1.MTOR_1,-30.7453699147
MDA-MB-361,CHK1.MTOR_1,22.1408482292
CAMA-1,MET_ALK.PDGFR_Ab,8.09927306595
MDA-MB-361,MET_ALK.PDGFR_Ab,-3.45355157314
```

Figure 3.4. Inspection of the head of exemplar output file of a single branch modelling, holding information on cell line, drug pair combination and finally value of produced prediction.

Not all feature vectors are processed in the same manner. This is espcially valid for a case of molecular and mono-therapy data where separate predictions are produced using global and local models.

3.3.1. Global models

What is considered as a global model is a model built on entire dataset available (Figure 3.5.). There are all cases and observations included, no filtering, subsetting or slicing of information is performed before.

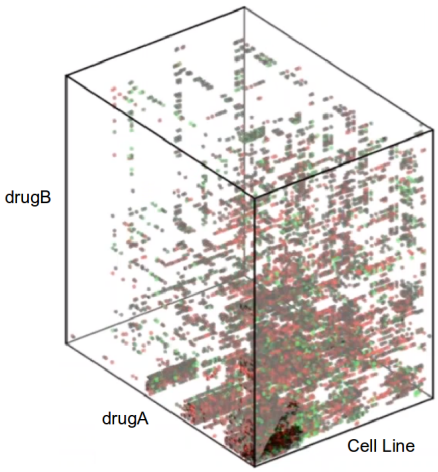

Figure 3.5. Visualization of 3D matrix with available data. All data points enter the global model to produce predictions.

There are three feature vectors proceeded with this approach: global molecular, global mono-therapy and chemical. Another characteristic of global modelling here applied, is that three separate runs are performed and the predictions are averaged to give the final outcome. In the case of molecular and chemical data, the training and test inputs are equal for the models, unlike for the mono-therapy step. Since the feature vectors are created with different orders of variables, those serve for creating individual training and test sets (Figure 3.6.). One of models is trained and tested on data sets constructed from feature vectors with the basic ‘A_B’ ordering. Another two share a common training set that encompasses feature vectors with both orderings: ‘max_min’ and ‘B_A’. Afterwards, they are tested on disjoint datasets created respectively from ‘B_A’ and ‘max_min’ vectors.

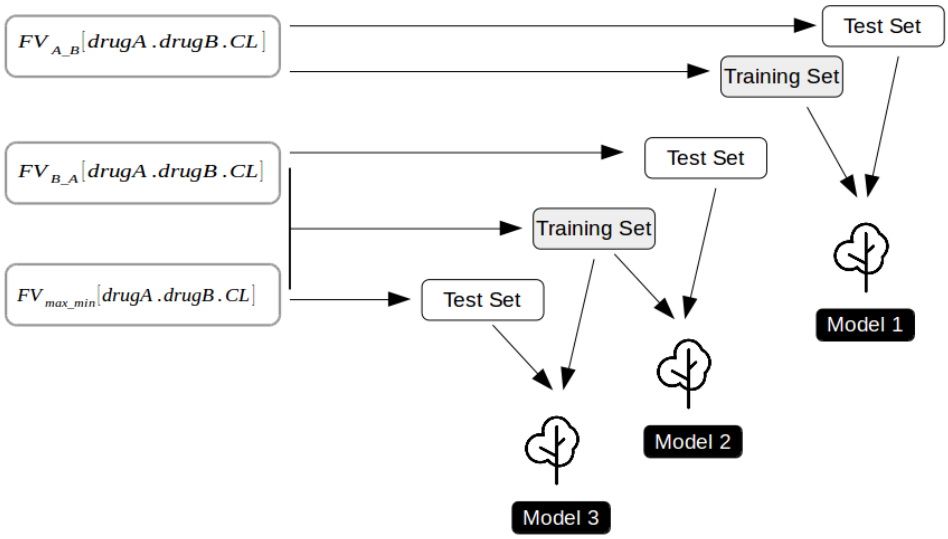

Figure 3.6. Visual representation of global modelling procedure performed for mono-therapy branch.

The individual models are joined by averaging four predictions, taking into account a duplicate of the last model outcome (3.25.).

$$P_{FVi} = \left(P_{Model\,1} + P_{Model\,2} + P_{Model\,3} + P_{Model\,3}\right)/4 \qquad (3.25.)$$

3.3.2. Local models

On the other hand, the concept of local models is to use for modeling just some part of the information. In practice it means, that in process of iteration among all drug pair – cell line instances, the separate small models are built and result in production of independent predictions. In the original implementation the local modeling approach is used for three feature vectors: file-counting and for two reproductions of global cases - molecular and mono-therapy.

Considering a single case of [drugA.drugB.CL] combination, firstly the chemical *A* serves as a 'slicing point' and the training set is created by selecting all the occurances related to this drug (Figure 3.7.). Model is trained and tested delivering set of predictions. In next step, the compound *B* becomes a filter and the training is performed on a dataset including only instances associated with this second drug. Modeling is repeated, resulting in new predictions. Finally the both outcomes are merged by averaging corresponding values.

The processing of local mono-therapy feature vector is a special case and requires additional comment. Although the data is sliced selecting planes of data corresponding to each of the drugs in the pair, the subsets are joined into a single one, and after proceeded similarly to a global version - for each feature vector order, the three separate models are prepared and merged (Eq. 3.25.).

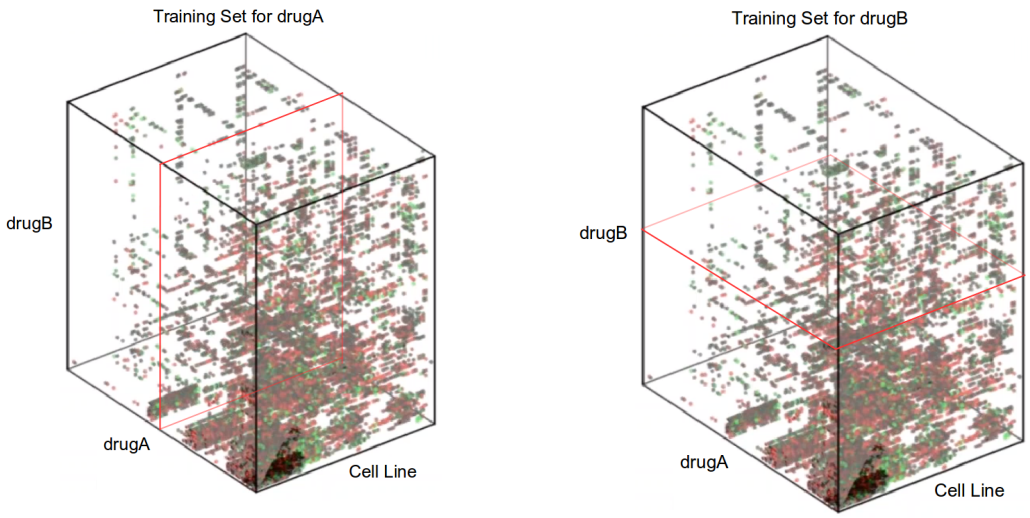

Figure 3.7. Visualization of data subsets created for each of the drugs from the considered pair in [drugA.drugB.CL] combination, that serve for building of local model.

3.4. Predictions

The response variable in the models is the total synergy score, drug pair – normalized. At first, it is not obvious why the outcome to be predicted cannot be directly an original value provided within the challenge data. To make it clear, the following simple example is recalled:

There are two schools, each with three classes of students. The task is to identify among both schools the pupils that are ‘good’ in performance in one particular subject.

But actually, when one can consider that the grade is ‘good’? When it is above some threshold? And if the level of education at the school is very high and it becomes difficult or impossible to get this score, shall the threshold be maintained? How to fairly compare the particular grades obtained in different circumstances?

The solution is normalization that would eliminate the variations corresponding to variables that are out of the scope of interest. What does it mean in practice? In this example, firstly the grades of students within the one class must be averaged and this value need to be subtracted from each individual score. The class-specific information becomes extracted and does not influence the outcome any more. The performance of students within the single school can be compared. Further, the procedure must be repeated but for pupils within a single institution: the school average is subtracted from each individual grade. In this way the values become comparable between the different educational environments.

How to identify which students performance is ‘good’? By comparing individual scores with a total average for all students from both schools. Values above the midpoint indicate the individuals performing better than the norm, while those scoring below the mean – the weaker ones.

Having this simple example in mind, let us turn back to the aim of this work and draw the analogy. The total synergy scores *SS*, computed according to the procedure described in section 2.1.1. Pharmacological Data, come from different contexts, reflecting the bahavior for different drug pair – cell line combinations. In order to make them comparable, they require to be normalized, as grades among different classes and schools. In the cohort of various assays, if we consider only a subset of trials carried on the same drug-pair (and various cell lines), the obtained scores must contain an ‘amount of information’ that is shared and equal for those tests. That is a baseline specific for an

applied treatment, that characterizes a compound-pair. Again, focusing on a subset of experiments run on the same cell line (and various treatments), produced values have common baseline specific for a sample under the drugs. This concept of synergy score decomposition (Figure 3.8.) allows identification of response variable that is a key value to be predicted through the established model. According to the ideia, those predictions compared with a total average value will permit determination of drug pairs with synergistic or non-synergistic effect.

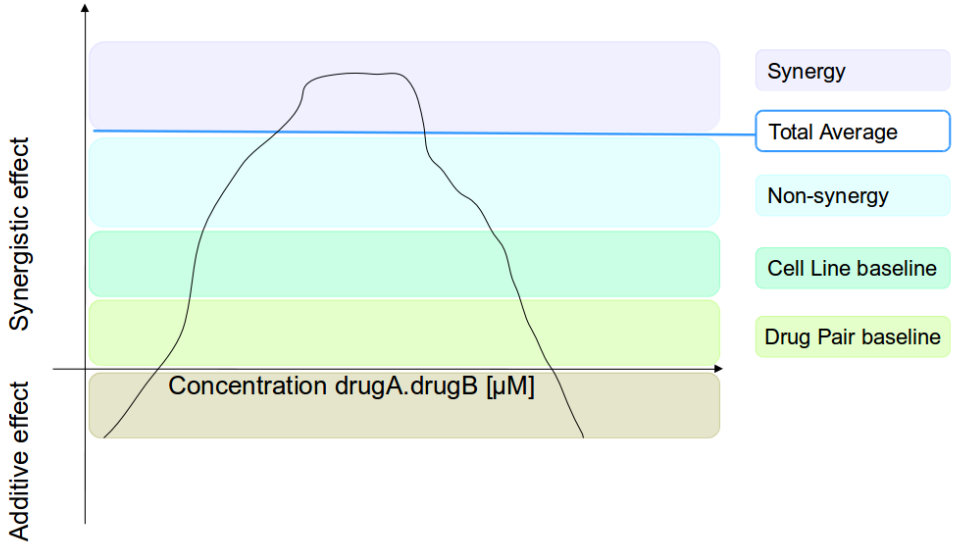

Figure 3.8. Visualization of an example of observed effect obtained in combinatory therapy for a drug pair - cell line combination and scheme of synergy score decomposition.

3.5. Merging

After producing six individual prediction sets from feature vectors described in section 3.2., all the outcomes need to be merged. The PERL script reads all the files with the partial results to separate dictionaries. Those consist of entries where the keys are tuples formed from cell line name and drug pair combination held in first two columns of each output record (Figure 3.4.). The value assigned to each of the keys is a prediction itself defined in third column of a file. The merge is completed by creating a single dictionary with all the test keys and respective final predictions, P_{final}, calculated from the partial outcomes by weighted averageing (Eq. 3.26.).

$$P_{Final} = \left(P_{GlobalMolecular} + 2 * P_{GlobalMonotherapy} + P_{Chemical} + P_{File\text{-}counting} + P_{LocalMolecular} + 2 * P_{LocalMonotherapy}\right)/4 \quad (3.26.)$$

The result obtained is saved in a *.txt* file with a standard structure, identical to partial output files (Figure 3.4.).

Finalizing, the second normalization is realized – regarding to a cell-line (see 3.4. Predictions) – to make the values comparable. The final results determining the predicted treatment effect, are organized in the matrix with the columns corresponding to the cancer samples, and the rows – to the unique drug combinations. Iterating all the lines, the total sum of outcomes and the number of all observations are calculated, allowing determination of the total average prediction value, $P_{TotalAvg}$. This value serves as a reference for identification of synergy. Thus, each instance is compared with $P_{TotalAvg}$, resulting in assignment of ‘1’ if the value is higher, and of ‘0’ otherwise. Thus, the final binary matrix indicates respectively the cases with predicted synergy and those with the null or antagonistic effect.

4. Implementation & Preliminary Results

4.1. Tools

The implementation of the machine learning model was accomplished using basically two programming languages namely Python and R. This work involved also acquiring of some knowledge and familiarity with the PERL (Practical Extraction and Report Language) since this is the language used in original scripts written by Yuanfang Guan. In submitted solution, the predictive models were generated applying the Random Forest algorithm by calling *TreeBagger()* function provided by MATLAB. The developed implementation used the same approach however it was adopted to R environment and employed with *randomForest()* function.

4.1.1. Python

Python is one of the high-level programming languages successfully combining efficiency and beginner-friendliness. According to the main goals of its designer, Guido van Rossum, it was created to be productive and readable. As broadly applicable (Web, GUI, scripting, etc.), interactive and open-source, it gains the popularity among all communities. It is portable and extensible, and allows object-oriented programming [43].

In this work, Python 2.7 was utilized to efficiently handle with large amount of information, especially on data pre-processing, simulation and integration steps.

4.1.2. R

R is a free programming language and environment, one of the most popular among statisticians, data analysts, researchers and market specialists. It provides utilities to retrieve, clean, analyze, visualize and report data. It was designed to be intuitive and to mirror the way the user think. It is interactive, vector-oriented and highly flexible language. R provides efficient utilities to handle missing values, almost impossible to avoid when working with real data [44].

In this implementation R 3.3.3 was used in data pre-processing, modeling and optimization steps. It was found very convenient and efficient due to the diverse functions that perfectly complemented the capabilities of the Python.

4.1.3. Random Forests

Random Forests (RFs) are powerful supervised prediction tool for classification and regression problems. The very first method of random decision forests approach was introduced in 1995 by Tin

Kam Ho and its increased accuracy was proved in the experiment on the recognition of handwriting digits [45]. It was later extended by including “bagging” and random selection of features [46][47].

RFs is an ensemble method, generating multiple fits and after all combining them to deliver improved results. The technique uses as a principal algorithm the standard decision trees, that separate the data into homogenous subsets, according to the most important splitter. The predicted feature is represented by terminal nodes or leaves, and the branches are particular sets of predictors driving to cohort division. In brief, the algorithm of growing decision trees takes all the root node data and scans through descriptors for the best splitter (that is: for the one providing the most pure children nodes). The one chosen divides the data and children nodes become parent nodes since the same growing step continues starting from them. The process continues until the terminal nodes are reached and the leafs include only homogenous subsets. However the individual trees built in greedy way are imperfect and can easily miss the optimal solutions (the splitting decisions are made locally, instantaneously without any general view on final outcome and without the possibility to change the past divisions).

Though the RFs idea is to take the collection of weak single tree fits, ensemble them and derive the final outcome by averaging or voting. There is a high probability that the obtained summarized model would be superior than any of the individual, and that it would be resistant to overfitting. The algorithm of generating RFs includes steps as follow. (1) Specification of the *N* number of iterations. (2) Bootstrap sample is picked from the original population with replacement. (3) Number of random descriptors is selected according to the value defined by user. (4) Independent, individual tree is grown on this subset. (5) Steps 1 – 4 are repeated *N*-times. (6) Collect all the trees and produce summarized outcome.

The RFs method was used in this work to create a baseline implementation reproducing the approach of Yuanfang Guan.

4.1.4. Server

This work was performed on server with Intel(R) Xeon(R) processor of number E5-1620V4. The processor base frequency of device was 3.50GHz while de number of cores – 8. It was equipped with RAM of 16GiB.

4.2. Outsourced Data

An additional prior knowledge was used in order to reduce the input size and to limit the data to the potentially most informative and relevant. It was achieved with catalog of the cancer driver genes and map of dosage-sensitive cancer genes.

4.2.1. IntOGen Mutations

In the development of the cancer there can be two types of alterations distinguished: driver, that contribute to the oncogenesis or that are relevant to the phenotype of the cancer, and passenger which accumulate through DNA replication but are not related to tumorigenesis. The Web platform IntOGen Mutations, provides a comprehensive tool for identification of cancer drivers. The database is built on the results of the systematic analysis of most currently available large data sets encompassing 28 tumor types among 6792 samples, including in the effect 1341752 somatic mutations [48][49]. There

are 498 cancer driver genes in a database among which some are more frequntly mutated than the others and which differ also in a scores that express the protein affecting mutations PAM (Figure 4.1.).

Figure 4.1. Cloud graph representing the most recurrently mutated cancer driver genes among total of 498. The font size is relative to the count of samples with PAMs – Protein affecting mutations, thus mutations that alter the function or synthesis of the protein product.

The platform uses for the driver identification Cancer Genome Interpreter[6] that carries the analysis relying on existing multi-source knowledge and on computational algorithms which annotate mutations considering different levels of evidence. The tool firstly detects the validated driver alterations and then classifies others of unknown significance using the OncodriveMUT method [50].

From IntOGen platform the *.csv* file with 498 cancer drivers was downloaded and served afterwards for filtering of original data source. The information is organized in a data frame with 4 field (Appendix 1E) providing repectively: HGNC symbol of gene, the specification and effect of alteration observed, and the probability assigned for determined driver role.

4.2.2. Copy Number Variation in Disease

The Copy Number Variation in Disease (CNVD) database[7] is a reliable and comprehensive tool that links the CNVs with multiple diseases. It served in this work as a base for filtering the genomic aberrations associated with cancer [51]. The database was built through text mining methods carried on original CNV-related papers published between 2006 - 2012 and downloadable from PubMed through EndNote software. The publications were manually analysed and the information on CNVs, associated pathologies, genes, chromosomes and other characteristics of aberrations was recorded and organized in Web platform. For the purpose of this work the *.txt* file listing tumour-related CNVs was retrieved from CNVD database after querying ‘cancer’ term. It has a structure of data frame with 13 fields (Appendix 1F) providing the standard identificator of CNV, the information on biological origin, localization in genome, specification of type, genes encompassed, eventual association with disorders, experimental metadata and PubMed references.

4.3. Pre-processing

As already mentioned before, majority of Guan’s scripts uses the input files different than the original provided within the challenge. The pre-processing steps producing the referred documents are not revealed by the author and they were inferred basing on scripts running further manipulations. The reconstructed procedures was performed in R environment.

[6] https://www.cancergenomeinterpreter.org/home; Last accessed on 22/05/2017;

[7] https://github.com/nkiip/GC2NMF/blob/master/0_origin_data/MGI_Gene.rpt; Last accessed on 22/05/2017;

4.2.1. Molecular Input

The objective of this step is to generate a set of six matrices corresponding to each molecular data source, with an unform organization. The respective matrices were saved in output *.txt* files holding the cell lines in columns and gene names in rows. Each of the original files required slightly different treatments and procedures since they were not uniquely structured, they dealt with various problems and demanded specific filtrations. Note, that this pre-processing steps are valid for both- global and local, molecular feature vectors.

RNA expression

While reading a *.csv* source file to a data frame in R, the attention must be paid since some slight automatic changes may occure in column and row names, as in the case of expression data source. The alterations took place for the cell line identificators strating with a numerical characters (they received a prefix '*X*') and for those containing hyphen sign within the name (hyphen turned dot). Those alterations are not severe however prevents the correct recognition and so needed to be fixed. After dealing with this feilure, the data frame was transposed to the requested standard conformation. Finally, two instances holding NA values were bound to the matrix, preparing the entries for cell lines for which expression data is missing (MDA-MB-175-VII, NCI-H1437) and would be imputed afterwards.

Copy number

According to the CNV definition in Genomics of Drug Sensitivity in Cancer[8], in order to consider a gene as amplified it needs to hold at least 8 copies, while to be recognized as deleted – no copy can be observed (the homozygous deletion, on both alleles). Following this interpretation, after reading a file to R working space, only the valid abberations listed in original CNV data source were selected. In order to avoid sex-dependent bias, additional filtering was performed and the alterations located on Y chromosome were excluded. Due to a large size of a data set and difficulties in handling, it was decided to limit the feature vector and include only the CNVs located in dosage-sensitive cancer genes. Those were determined using as areference the file outsourced from the Copy Number Variation in Disease (CNVD) database (4.2.2. Copy Number Variation in Disease). The final molecular matrix was generated and the data was binarized assigning to each gene - cell line combination a CNV status: '0' corresponding to an absence of an aberration and '1' standing for a presence of 1 or more CNVs.

DNA sequence

Again, preselection of relevant genes was necessary to achieve construction of realizable implementation. Thus, only the mutations located in the driver genes were included in generation of molecular matrix. This filtering was performed according to the file outsourced from the IntoGen platform (4.2.1. IntOGen Mutations). Secondly, the irrelevant mutations were excluded by removal of the instances assigned in the original source file with 'PASSENGER/OTHER' status in FATHMM prediction, and those identified as 'Confirmed somatic variant'. The binary matrix was created similarly to CNV case - by assignment of the mutation status to each gene - cell line: '0' corresponding to an absence of a variant and '1' standing for a presence of 1 or more mutations.

DNA methylation

The pre-processing of the methylation data source initialized with the assignment of the genes to the probes and removel of instances without genetic annotation. As in the case of expression file, the cell line names required corrections due to an automatic modifications introduced by R. Another issue – presence of multi-gene probes, was solved by multiplication of those instances by the number of assigned genes and identification of each entry with a single gene annotation. The data frame was

[8] http://www.cancerrxgene.org/; Last accessed on 27/09/2017;

transposed to create a matrix with a standard structure. It was extended by three instances holding NA values for missing cell lines (MDA-MB-175-VII, SW620, KMS-11) that served for future imputation.

CCLE RNA expression

In order to generate standard matrix summarizing expression data provided by CCLE, the instances in original file were assigned with the genes and than filtered retaining only the probes with the annotations. The automatically introduced failures in cell line names were corrected turning the identificators consistent with the Sanger nomenclature. The data was subset selecting only the information related to cancer samples included in experiments. Three instances holding NA values were introduced to the data frame, simulating the entries for missing cell lines: M14, MFM-223, NCI-H3122. One of the genes, TTL, was found to be assigned to two different probes. The issue was overcome by keeping a single instance with a median value.

CCLE copy number

After the reading of an original file to a data frame in R, a correction step was required to obtain HGNC standarized cell line names. The instances corresponding to the cancer samples covered by the challenge experiments were selected. As for CCLE expression data source, value for the same set of cell lines is unavailable: M14, MFM-223, NCI-H3122. Thus, the molecular matrix is extended by three entries holding NAs for posterior imputation.

Both datasets outsourced from CCLE required additional pre-processing step, run in Python, translating the internal nomenclature of sample to normalized primary cell line names. The conversion was performed using as a reference *.txt* file outsourced from the CCLE platform, that contains cell-line metadata from the cancer lines used in drug sensitivity screens.

4.2.2. Pharmacological Input

As one of the inputs for the mono-therapy feature vector serve the *.csv* files on the experimental results of the single-compound assays (see 2.1.1. Pharmacological Data). The number of files storing the data is higher than the number of drug pair - cell line combinations tested. The reason is that some of the trials were repeated several times due to the problems in the performance. The accurate determination of experimental file of origin for each of instances was a challenge. Different approaches were undertaken: determination by quality score, by exclusion, by manual curve-fitting etc. but none achieved to unequivocally identify the correct data source. The reproduction of dosage-response curve fitting performed automatically with Combenefit software was not attained. Due to this issue, it was decided to exclude the multi-source observations since those could introduce bias to the model. Thus, 123 of total 2199 drug pair - cell line combinations were not included in further processing, and feature vectors were constructed basing on 2076 unambiguous cases.

4.2.2. Compound Input

The input file holding information on chemical and structural drug characteristics (2.1.3. Compound Data) deals with large amount of missing data: among 119 observations only 58 contain complete information. Firstly, it was tempted to estimate the unavailable values basing on known measurements of the most similar compounds, averaging them. However, this approach was not efficient and since the *rfInput()* function of R provides far easier solution and much better outcome, it become implemented in script. No other pre-modelig steps were required for this data source.

4.4. Modeling

As presented along pre-processing, the missing cell lines were introduced by appending the instances filled with NA valaues. This approach is afterwards complemented by utilization of additional R function – *rfImpute()*, just before building the model in order to simulate missing data using proximity from randomForest. It was convinient solution since both maipulations are performed in R environment but being jointly called from a Python script. This approach provided better results than other experimented: imputation based on the averaging of values found in set of the most similar cell lines. The similarity was determined by computing the distances between samples basing on available molecular data.

Originally the models were created using random forest algorithm and the approach was reproduced in this work applying analogous *randomForest()* function that belongs to the R package of the same name [52]. It is an implementation of Breiman's random forest algorithm established on Breiman and Cutler's original Fortran code, for both classification and regression problems.

The number of trees grown was set to 200, following the original value of the argument. The first variable in data was used as the response and resting are predictors. The outcome variable was - equally to the winning solution - normalized synergy score. The predictions were saved in *.txt* files with the structure identical to the standard proposed by Yuanfang Guan.

The baseline implementation exactly replicates the original steps of generation of partial and final models, as well as the merging procedure.

4.5. Evaluation Metrics

In order to evaluate the process of reproduction of winning solution and to assess the performance of baseline implementation, the set of five different metrics were used. They all are used to determine the goodness of fit of machine learning binary classification models. On the purpose of this work, the following terminology was defined:

TP – number of true positive occurences,

FP – number of false positive occurences,

TN – number of true negative observations,

FN – number of false negative observations.

Matthews correlation coefficient (MCC)

Introduced by biochemist Brian W. Matthews [53], the MCC metric expresses the correlation coefficient estimated for the true observation and respective predicted value. It is considered as reliable and balanced, having a special characteristics – being immune to differences in class sizes [54]. The computation is performed basing on true and false positives and negatives (Eq. 4.1.). Its value varies between -1 and +1, indicating in the first case the total inconsistency among predictions and true values, and the pefect match – in the latter. Value equal to zero suggests that the model predictions are random.

$$Matthews\,Correlation\,Coefficient\ MCC = \frac{TP * TN - FP * FN}{\sqrt{(TP+FP) * (TP+FN) * (TN+FP)(TN+FN)}} \quad (4.1.)$$

Sensitivity

This metric is also known as true positive rate, recall or probability of detection, depending on the field where is applied. Its value represents the proportion of positive instances correctly dermined by the model (Eq. 4.2.) [54]. The sensitivity can be interpreted as manner of quantification of avoiding of false negatives.

$$Sensitivity = \frac{TP}{TP + FN} \quad (4.2.)$$

Specificity

Another popular denomination of this metric is true negative rate and it is just opposite to sensitivity. It expresses the proportion of negatives observations correctly indicated as such by the model (Eq. 4.3.) [54]. Analogously, it provides a manner of quantification of avoiding the false positives.

$$Specificity = \frac{TN}{TN + FP} \quad (4.3.)$$

Accuracy

The difference between a prediction and a true value can be expressed by accuracy. It is a ratio of all observations correctly identified by model total number of instances (Eq. 4.4.) [54]. This metric reflects how close the estimations and observations are. Although, very informative, the accuracy is sensitive to imbalances in classes sizes (that is a case of this work).

$$Accuracy = \frac{TP + TN}{TP + TN + FP + FN} \quad (4.4.)$$

Balanced Accuracy

In some circumstances accuracy estimate may become more optimistic then the reality is. To overcome this issue more general metric may be used – balanced accuracy, that is simply the the average accuracy obtained on either class (4.5.) [55].

$$Balanced\ Accuracy\ BAC = (\frac{TP}{TP+FN} + \frac{TN}{TN+FP})/2 \quad (4.5.)$$

4.6. Results

As mentioned in the introduction, after establishing the functional baseline implementation, the work was presented to a small public, in order to reflect on obtained results and to determine further directions.

The model was evaluated including the specific feature vectors one by one. The reason for this approach was to monitor the behavior after single inclusions and to have an idea on impact that each of the specific data source has on the overall outcome. Moreover, the generation of predictions was a time-consuming process, especially in the case of molecular data sources so the results were produced gradually. The predictions created on local molecular feature vectors were never obtained throught the baseline implementation – the run was killed after 2 weeks of processing. The results are summarized in table 4.3.

Table 4.3. The partial result of evaluation of baseline implementation.

Model	MCC	Sensitivity	Specificity	ACC
Global Molecular	0.62637	0.63212	0.97828	0.95589
+ Chemical	0.61702	0.63007	0.97683	0.95449
+ Global Mono-therapy	0.73367	0.74397	0.98353	0.96804
+ File-counting	0.71282	0.71780	0.98297	0.96581
+ Local Mono-therapy	0.74383	0.76398	0.98304	0.96887
+ Local Molecular	n/a	n/a	n/a	n/a

Some conclusions may be formed basing on the data presented above. Firstly, apparently the inclusion of chemical and file-counting data hurts the model causing a drop of all evaluation metrics. The best scores are obtained after including the predictions originated from a local mono-therapy feature vectors – this step boost the model.

Generally the values are optimistically good. Investigating the reason of observation such high scores, the failures and imperfections of the experiment design were found. It must be reminded that this results were obtained testing a model on the original test set from the challenge. This fact implies that, since true values had not been published yet, the implementation was evaluated using as a reference matrix the final outcomes submitted by Yuanfang Guan, assumed as a ‘true’ on the purpose of this work. Moreover, the assessment was performed including all the possible combinations, while the ‘0’ values indicating non-synergic effect were assigned also to the unknown cases. That means that the number of true negative is falsely elevated and the values obtained for specificity proves it.

According to this conclusions it was decided to on the purpose of this project construct a new training and test sets, from the available and known challenge data. The new subsets had to reconstruct the original circumnstances what in practice meant that they had to be totally disjoint on drug pairs. They were balanced in size, holding 30% and 70% of data by respectively test and training sets.

It was decided that in order to obtain reliable evaluation scores the model assessment must be performed exclusively on the test instances, neverthless that an entire matrix holding all possible combinations is produced. The alterations were introduced into the script and the unknown cases although still present in prediction matrix, they become to be assigned with NA values.

Furthermore, three directions of future work to be developed were defined:

1) Feature selection;

2) Alternative models;

3) Predictions-merging equation.

5. Model Improvement

Since the molecular data source deals with abundance of variables, the main point of the focus was to reduce the number of features included in the model selecting only the informative ones. The aim was also to determine the most important variables because those could be the potential biomarkers.

The baseline implementation follows the winning solution building the models with Random Forests algorithm. However there is no evidence provided by the Yuanfang Guan that this approach is the most proper for the challenge problem. In this work an efforts were made to test the performance with two others methods: Support Vector Machine (SVM) and Multivariate Adaptive Regression Splines (MARS).

Moreover, the attempts were also directed at establishment of optimal merging equation since no information is available confirming that the version implemented in original script is the most accurate one. The establishment of used coefficients is not reported in the submission documentation, neither in PERL scripts.

5.1. Feature Selection

Feature selection in machine learning approaches is very often a requisite step for model building. Nowadays it is necessary to deal with large datasets with many variables since the production of the data is rather not an issue anymore. This fact brings two complications:

1) most of the variables are not relevant, they do not contribute to the model or even can cause a decrease of accuracy. Those preferably should not be included in the feature set at all.

2) high technical requirements. Large datasets are demanding to deal with because they highly slow down the process and may turn it impossible to run in reasonable time. Also they need many resources that are often unreachable for one.

Thus it is preferable to select possibly the smallest set of variables that would ensure the optimal results and manageable data size. It is necessary to find an approach that would identify all of attributes with their relevance to the model, indicating those that shall be retained and included in the process.

5.1.1. Tools

Least Absolute Shrinkage and Selection Operator

Least Absolute Shrinkage and Selection Operator (LASSO) is a supervised regression machine learning method using a shrinkage [56]. The approach generates simple and sparse models, especially

convenient in the case of high multicollinearity among variables where only most important features are selected.

The principle of the lasso is shrinkage that is in general bringing down of values to some central point. Since the method requires a constant threshold defining the maximum sum of the absolute model parameters, it implies that some variable coefficients would be reduced to 0. In the effect the shrunk model will include fewer features, those for which the coefficients remain different from 0. The features selection step allows to determine the predictors highly associated with the respond variable and minimizing the error related to the outcome. Also, due to such a simplification, the interpretation of model becomes improved and user-friendly. The lasso is able to provide models of high accuracy and is especially useful when there are relatively low number of instances and high number of predictors.

The simplicity of lasso regression is also in a tuning by a single parameter λ, that controls strength of the penalty. The higher value of parameter, the more reduced model is obtained what means that more coefficients are turned to 0.

Boruta

Boruta is an ‘all-relevant’ wrapper algorithm for feature selection through the variable importance measure (VIM) [57]. It identifies variables correlated with the response more than random ones. By default it is built around the random forest classification but the function is able to work with any other method for which the importance metric is available. In short, Boruta selects the relevant features comparing their original importance with the random estimations from permuted copies. The search is run top-down and irrelevant attributes are eliminated gradually.

The idea of approach was inspired on RFs methodology where the randomness is introduced to the analysed system and the results are obtained from an enseble of samples picked by chance [58]. In this way the added randomness reduces the tricking influence of casual variations and non significative correlations, and meanwhile it is supposed to expose the truly important features. The main steps of algorithm include: (1) The system is enriched with extra copies of all attributes (so called *shadow features*). (2) The added variables are shuffled removing the random correlations. (3) The default RFs classification algorithm (applied here due to its quickness, no need for parameter tunning and the output of numerical estimation of importance) is run and the VIM values are obtained for enriched data (mean decrease accuracy by default). (4) For each attribute, the Z- score is compared with the maximum value observed among all its shadow features. If scoring significantly higher, the variable is recognized as important and kept in data system, otherwise it is assigned as non-informative and permanently eliminated. (5) The procedure is repeated untill all the attributes are identified with confirmation/rejection status or when the limit of RFs runs is reached.

5.1.2. Methods

Overall, the establishing of feature selection approach for molecular data sources was one of the most laborious stages of the project. The workflow was changed and adjusted along the progress. The final procedure is visualized graphically on figure 5.1. and described in details within the following sections.

The various attempts were performed to define the set of the most informative features with Boruta algorithm. However, the methodology was found inconvenient in this work due to inconvinient relative values expressing the importance and low reproducibility of results with such a high number

of variables. One of the experiments run with this methodology had as an aim the establishment of significance order for all molecular branches. In the result the global models built on mono-therapy and molecular data sources were identified as the most relative. Next in the order were their local adaptations, after - the counting-file branch, and finally determined as the less important – chemical data source. Those indications were taken into consideration while optimizing and establishing new values of coefficients in equation merging the branches.

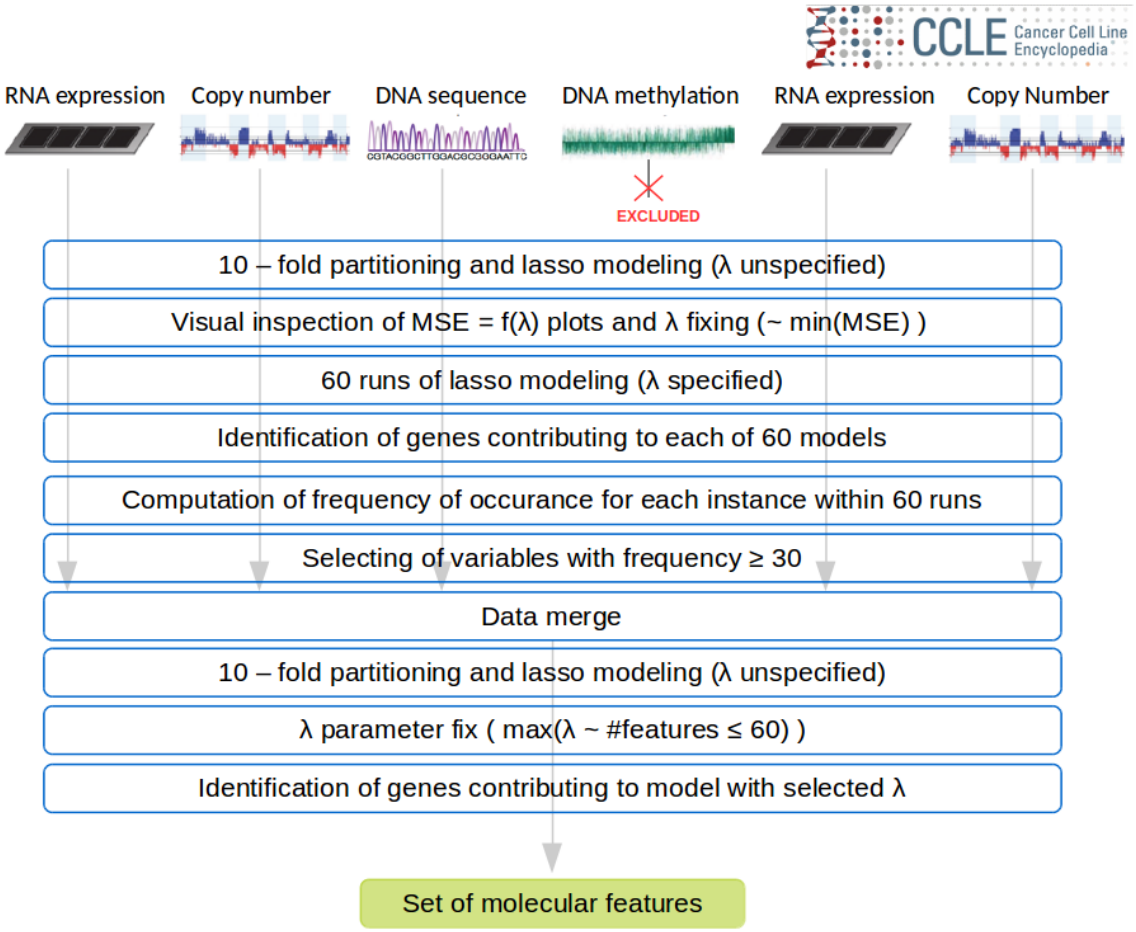

Figure 5.1. Workflow of feature selection performed on molecular data sources applying Lasso algorithm.

Pre-processing

To start, for different molecular data sources the separate files are prepared in Python. The process is similar to one implemented in baseline approach. The only difference is that instead of assigning feature vectors to cell lines [CL], they are directly attributed to corresponding response values, i.e. normalized synergy scores that are going to be predicted by afterwards created models. Thus, the *.txt* files produced for molecular data sources follow the standard structure where first column of each line is an outcome value and the next – predictor variables determining state of each particular gene. The features selection is performed for five of six sources: gene expression, CNVs, mutations and two CCLE outsourced files. The methylation is excluded due to the size of dataset that turns procedure unrealizable in acceptable time.

Selection

This step is realized in R and processes each of molecular information source separately. It starts with data partitioning and creating of 10 disjoint folds of the same size. In each iteration one of subsets serves as test set while the rest makes the collection of training sets. The model is created with *glmnet()* function of a R package of the same name [59], which fits a generalized linear model (GLM) with lasso regularization since a parameter alpha is set to '1'. The fitting is realized via penalized maximum likelihood and the sets of estimations are computed for different values of the regularization parameter lambda. Next a grid of the predictions is produced for a range of considered λ. Those are compared with the true values in a test set and for each parameter λ a mean squared error (MSE) is calculated.

After terminating a loop, a data frame summarizing runs for all data folds is generated. Each run is characterized with a list of lambda parameters and corresponding MSE values. In order to select the most advantageous model, the *.png* image is created with a graph summarizing the runs (Figure 5.2.). Each curve plots the lambda as a function of mean squared error: *MSE = f(λ)*. The lambda parameter values are presented on X-axis while computed corresponding mean squared error – on Y-axis. The visual inspection of a graph allows estimation of a parameter λ that potentially could bring the most promising result.

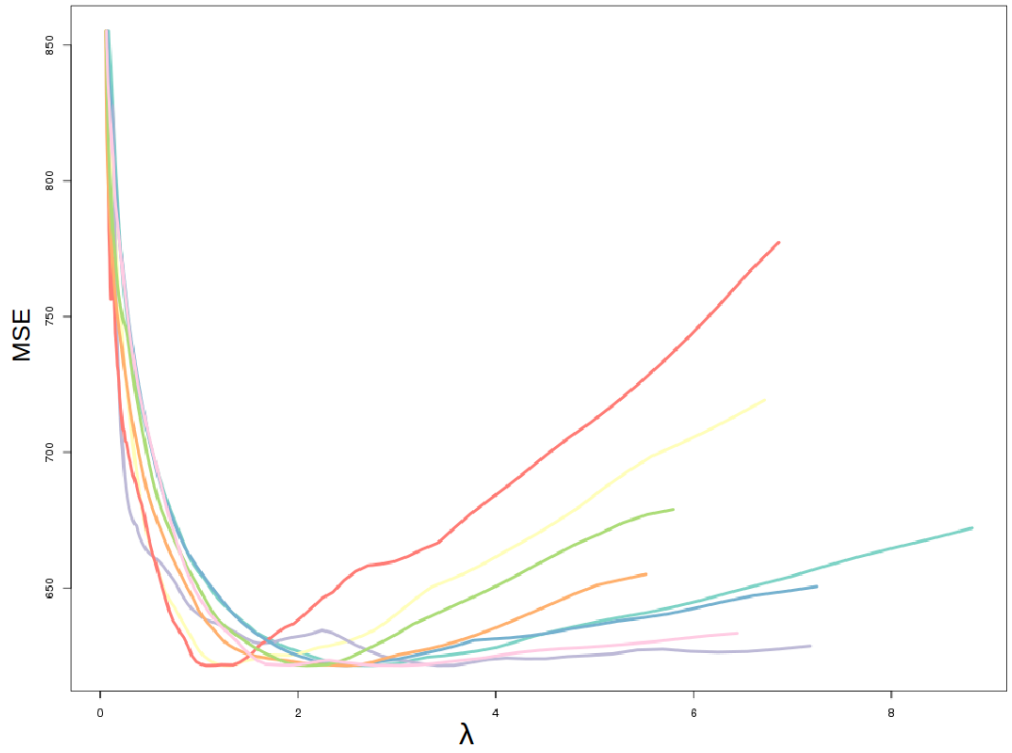

Figure 5.2. Graphical summary of example predictions produced by lasso models for gene expression data. Each curve plots the mean squared error as a function of λ: *MSE = f(λ)*. The lambda parameter values are presented on X-axis while computed corresponding mean squared error – on Y-axis.

The graphical visualization prepared for each molecular data set allows establishing of a final set of lambda parameters (Table 5.1.).

Table 5.1. Values of lambda parameter established after the visual inspection of summarizing plots.

	Gene expression	CNVs	Mutations	CCLE expression	CCLE CNVs
λ	2.00	1.50	1.25	2.00	1.00

Subsequently, an entire data set is divided to training and test set containing respectively 70% and 30% of original information. Again a lasso model is prepared but this time with a determined λ parameter. Having a lambda fixed it is possible to obtain the coefficients assigned to variables and determining their contribution to the selected model. At this point the genes that has coefficients different from 0 are considered as important for obtaining possibly the best predictions. The set of three steps described above: 1) data partition, 2) fixed λ model building and 3) determination of informative variables, they are repeated in 60 independent runs. The lists of selected features are merged and for each instance the frequency of occurence is calculated.

It is assumed that if a gene appears repeatedly (for example 50 times) within 60 runs, this fact shall reflect its importance in the model. Contrary, if some instance was observed only once or two times, it can be clearly presumed as an occurence by chance. According to this logic, a particular threshold that determines a frequency of relevant events, needed to be established.

The threshold is set to 30 for all of data sources, after plotting mean squared error as a function of a number of features: *MSE = f(#features)*, for all the selection of produced models (Figure 5.3). The number of variables in model is presented on X-axis while corresponding mean squared error – on Y-axis.

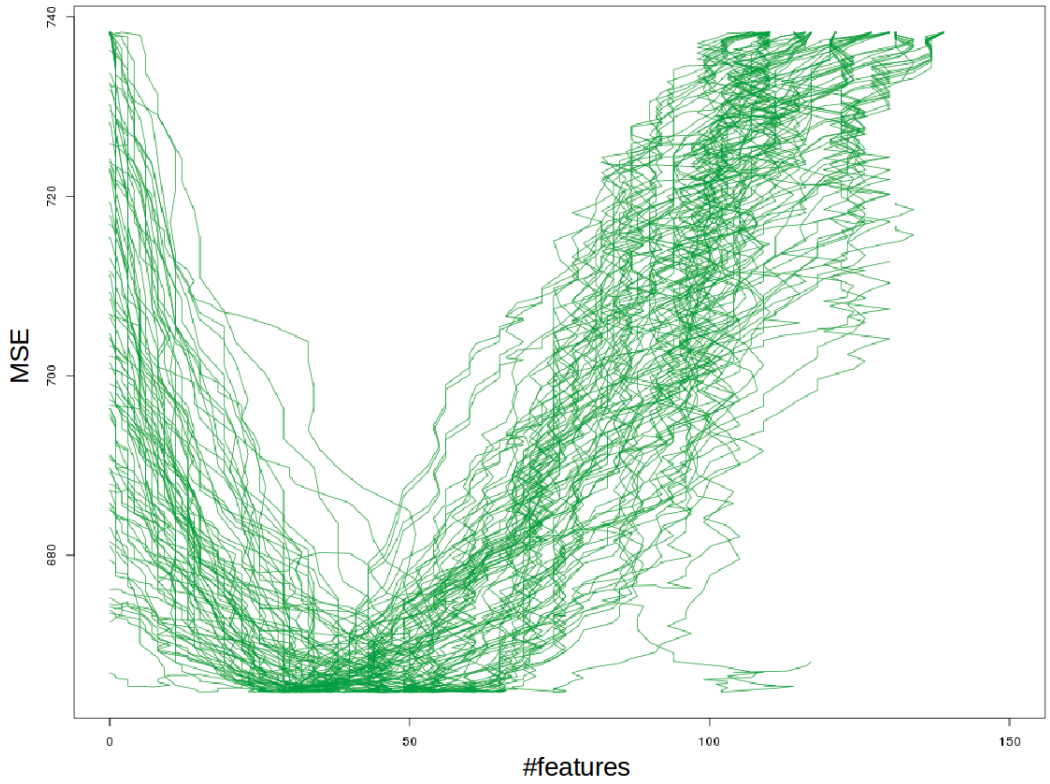

Figure 5.3. Visualization of predictions produced by lasso model on molecular data with features selected according to the established workflow. Each curve plots the mean squared error as a function of number of features: *MSE = f(#features)*. The numbers of features are presented on X-axis while computed corresponding mean squared error – on Y-axis.

As the graph suggests, there is no point in building a model on more than 50 features – inclusion of next variables does not bring an improvement. Thus, defined cut off on frequency allows selecting from each data source less than 50 variables as summarized at the table 7.2.

Table 5.2. Summary of the number of features selected on each data source with lasso algorithm, with the frequency of occurance at least 30 per 60 runs.

	Gene expression	CNVs	Mutations	CCLE expression	CCLE CNVs
# features	31	33	29	25	47

The figure 5.4. summarizes the result of 10-fold cross validation run on model with a frequency threshold set to 30. Light blue plots correspond to each run while navy blue curve averages the outcomes. According to the graph, the lambda parameter with a value around 2 shall provide results with reduced MSE.

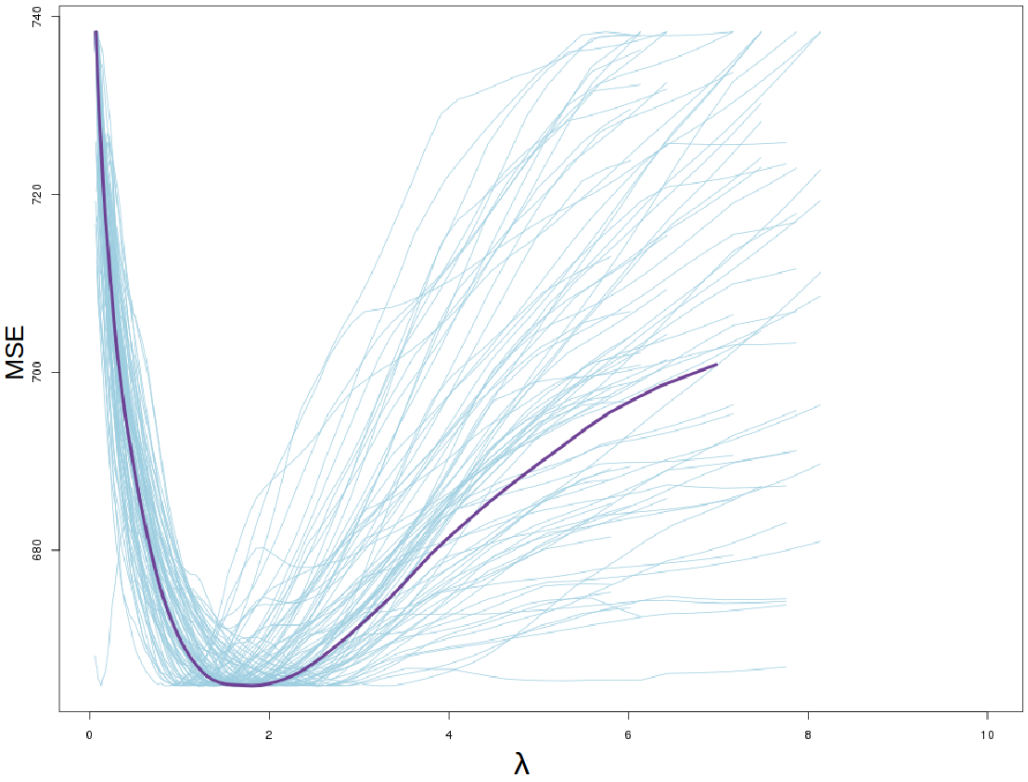

Figure 5.4. Visualization of predictions produced by lasso model on molecular data with features selected according to the established workflow. Each curve plots the mean squared error as a function of lambda: *MSE = f(λ).* The lambda parameter values are presented on X-axis while computed corresponding mean squared error – on Y-axis.

Next, the produced gene lists are merged in unspecified order and for each partially normalized synergy score a feature vector holding in total 165 variables is created. Again, the generated dataset is partitioned into 10 disjoint folds, where in each iteration one of those serves as test set while others – as collection of training sets. The lasso models are created without fixed lambda parameter. The grid is generated that holds for each run: λ values, corresponding mean squared errors and respective number of features entering the particular model. This data frame serves for final determination of lambda. Thus, the value of parameter is fixed to a maximum λ providing a model built on 60 or less features. Obtaining coefficients assigned to variables for defined lambda in the last created lasso model, the list

of potentially most important features is defined. This collection is included in pre-processing step of global molecular branch as a filter on already simulated feature vectors, allowing reduction of their size and selection only of variables detected as informative.

5.1.3. Evaluation

It was decided to observe the behavior of an established feature selection workflow in order to confirm its ability and productivity by graphical visualizations. Particularly it was pretended to verify if MSE and lambda parameter values obtained during the process of establishing a feature selection workflow are reliable or rather could be observed by chance. The simulation generating 500 lasso models with selected features allows inspection of distribution of minimum MSE produced within all the runs and their corresponding lambda parameters, as presented on the figures 5.5. and 5.6. respectively.

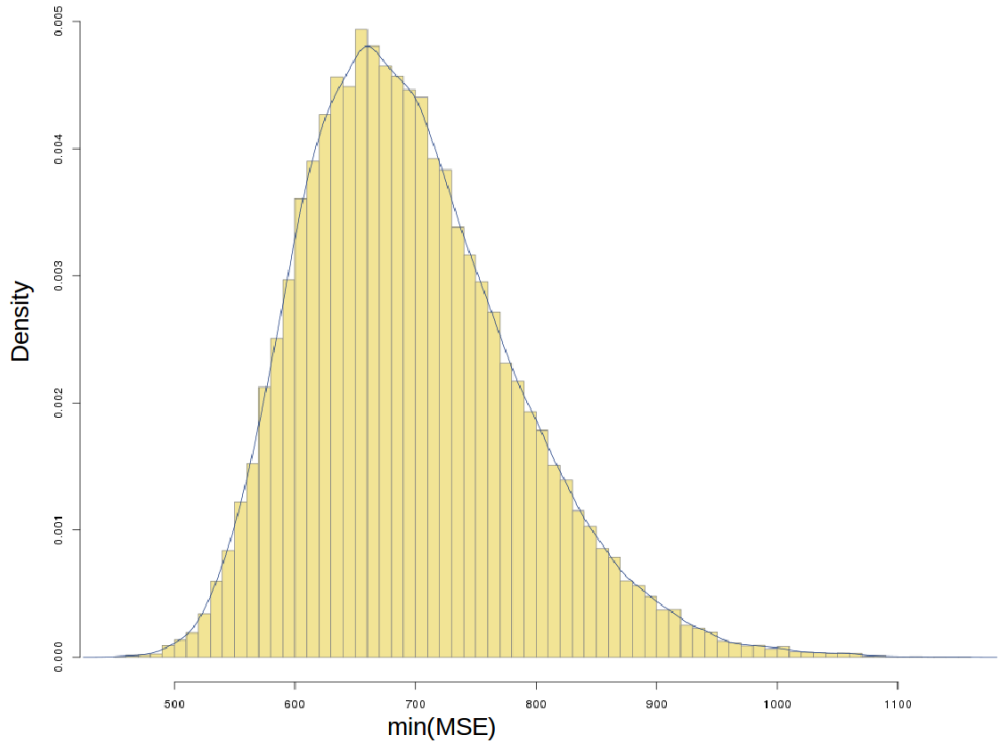

Figure 5.5. Histogram of minimum MSE values obtained in simulation of 500 runs.

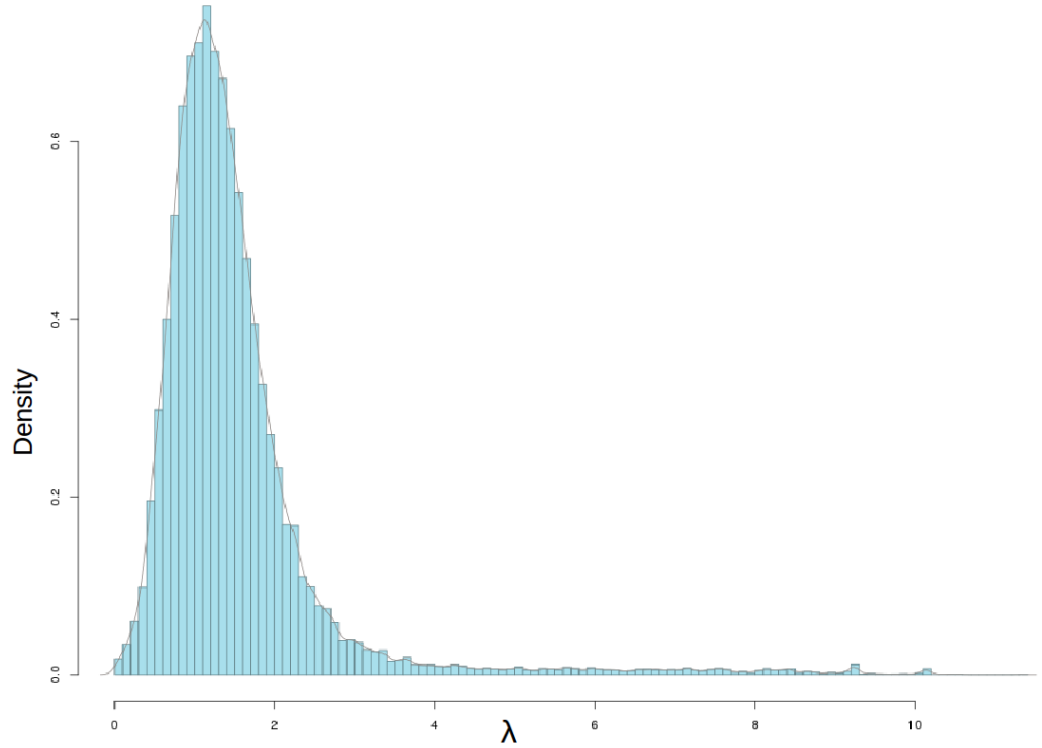

Figure 5.6. Histogram of lambda parameter obtained for minimum MSE values produced in simulation of 500 runs.

Both graphs confirm that small models obtained during the establishing process somehow reflected the general trend in the data and so it can be relied on.

5.2. Regression Modeling

5.2.1. Tools

Support Vector Machines

Support Vector Machines (SVM) is a non-linear supervised learning algorithm applicable in classification and regression problems. Although it was developed in the 1990s by Corinna Cortes and Vladimir Vapnik [60], it still continues to be one of the most popular and efficient methods, recommended especially for data with numerous variables.

The idea of SVM is to create a separating optimal hyperplane (or a set of those in high-dimensional space) that would - perfectly - to any given instance assign a correct category. The unique and the best solution is found for the maximum margin of the training set (convex optimization – no local minima). Often the hyperplane cannot be defined by a linear equation and the *kernel trick* must be applied. That is, using nonlinear mapping, the original data is transformed into a higher dimensional space, in such a way that allows creating linear decision boundary within instances. Among most common examples of kernel functions applied in practice, the polynomial, radial or sigmoid are found.

In this work SVM was experimented as a machine learning methodology in a process of optimization. It was chosen due to its robustness, high prediction accuracy and low overfitting. Although it is computationally expensive and slow, still it is expected to exceed the performance of RFs [61][62].

Multivariate Adaptive Regression Splines

Multivariate Adaptive Regression Splines (MARS) is a nonparametric supervised learning algorithm for regression and classification problems, that does not require any assumption about relationship between predictors and the dependent variable. The existing correlations and functions are derived on the basis of the original data. The general idea is to divide total data space and obtain groups of instances for which the local regression equation may be determined [63][64]. This is s reason why MARS is suitable for large inputs, overcoming limitations of many other machine learning methodologies.

The algorithm includes following steps: (1) generation of simple model with the constant basis function; (2) exploration of basis function space, with all possible variables and knots; (3) selection of solutions that provide the best model (those with minimal prediction error); (4) repetition of search-select steps (3 and 4) until the pre-defined complexity limit is achieved; (5) pruning eliminating solutions with the least contribution to the total goodness of model [65].

MARS being very promising, especially in complex data mining problems, was chosen to be experimented in the model optimization and compared to the RFs and SVMs performance.

5.2.2. Methods

Regarding to the Support Vector Machine, it generates the models using *svm()* function provided within '*e1071*' R package [66], that is based on implementation by Chang et al. [67]. In general, the concept follows a sequence of steps:

1) Class separation – having two classes, the optimal separating hyperplane is established, always aiming the maximization of the margin between the closest instances of the two sets;

2) Dealing with overlapping classes – the instances that are incorrectly classified with built hyperplane are weighted down in order to minimize their impact;

3) Handling the nonlinearity – if the instances initially are not linearly separable, they are projected via kernel techniques into an higher-dimensional space, allowing construction of linear separator;

4) Problem solution – known techniques are adopted to solve a final quadratic optimization problem. [60]

An another experiments were carried implementing a Multivariate Adaptive Regression Splines (MARS) approach for building a model. The *earth()* function from R package of the same name [68] was utilized and a regression model was generated basing on Friedman's techniques [69].

Although both algorithms surpass a Random Forest approach, always the SVM methodology is in a favour and brings the improvement into the final model.

5.3. Prediction-merging equation

The merging step reconstructed on original implementation of Yuanfang Guan, follows the general equation presented already in section 3.5. and recalled below:

$$P_{Final} = \left(P_{GlobalMolecular} + 2 * P_{GlobalMonotherapy} + P_{Chemical} + P_{FileCounting} + P_{LocalMolecular} + 2 * P_{LocalMonotherapy}\right)/4$$

Thus, the originally applied coefficients are set to 0.25 for four branches: global and local molecular,

chemical and file-counting, while they are equal to 0.5 for both mono-therapy data sources. In this work an attempts were undertaken to optimize the merging equation and different versions of computations were performed varying coefficient values between 0 and 2, in various combinations. Observation of the parameters and their final outcomes for chosen SVM model, allows establishing of the most efficient values. The identified coefficients are summarized in the optimized equation 7.1.

$$P_{Final} = \left(2 * P_{GlobalMolecular} + 0.25 * P_{GlobalMonotherapy} + 0.25 * P_{Chemical} + 0.25 * P_{FileCounting} + 0 * P_{LocalMolecular} + 0.25 * P_{LocalMonotherapy}\right) \quad (5.1.)$$

6. Results & Discussion

Although there is a test set provided within the challenge, it could not be utilized as such in this work since the true values are unavailable. Thus, it was decided to independently create training and test subsets from a data with known synergy scores. The aim was to reproduce as accurately as possible the original training and test environment and the relation between two subsets.

It was observed that provided training and test drug pairs are disjoint – none of the training compound combinations is present in a test set. Regarding to the size, the test set is approximately two times smaller than the other. While it is understandable to follow the first indication and mimic it creating cohorts independent in drug pairs, it was found unreasonable to reproduce the size proportions. The general rule of machine learning was followed and standard partition was performed: ~ 70% of data became training set and resting ~ 30% - a test.

In the effect, the final implementation was trained on the dataset of 4434 observations encompassing 378 unique drug pairs, and tested on 1898 cases with 161 unique compound combinations.

Established feature selection workflow allowed production of a list with molecular variables identified as informative and contributing to the model. In total, 75 features were determined, including between 8 and 19 from particular data sources as summarized in the table 6.1. The total list of selected features is provided in Appendix A.

Table 6.1. Summary of the final number of features selected on each data source with established and applied feature selection workflow.

	Gene expression	**CNVs**	**Mutations**	**CCLE expression**	**CCLE CNVs**
# features	17	12	19	8	19

The final optimized implementation was run using as a model building algorithm Support Vector Machine within '*e1071*' R package, and merging the branch models according to the equation 7.1. In the table 6.2. the final evaluation results are presented, following the metrics defined in section 4.4.

Table 6.2. The final result of evaluation of optimized implementation. Values are averages from three identical and individual runs.

MCC	**Sensitivity**	**Specificity**	**ACC**	**BAC**
0.985	0.708	0.789	0.631	0.847

Those values can be referred to the evaluation results obtained in 3rd submission of original implementation by Yuanfang Guan. The scores recalled in table 6.3. are published in a DREAM challenge website, section 4.2 – Subchallenge 2[9]. For the final submission only the BAC metric is known: 0.61, indicating that the performance was slightly weaker than for a leaderboard.

Table 6.3. The evaluation scores obtained by Yuanfang Guan in the 3rd submission, performed on the subchallenge 2 leaderboard.

MCC	Sensitivity	Specificity	ACC	BAC
0.27	0.71	0.6	0.35	0.66

According to presented metrics, the performance of optimized implementation being an objective of this work, provides better results than the original inspiration approach.

The list of features selected in process of optimization brought an interesting matter to explore more and study. The selection of 75 variables includes 3 genes that are relative to model due to two molecular characteristics each (Table 6.4.). Those and more 11 genes of the final selection, are targets according to the list provided within the challenge.

Table 6.4. Genes within features selected in optimization process which contribute to final model with more than one molecular characteristics. The aliases are determined according to GeneCards Human Gene Database (www.genecards.org).

Gene	Molecular Characteristic	Aliases
ATR	mutation & expression	ATR Serine/Threonine Kinas
MAP2K1	expression & CCLE expression	Mitogen-Activated Protein Kinase 1
XIAP	expression & CCLE CNV	X-Linked Inhibitor Of Apoptosis, E3 Ubiquitin Protein Ligase

One of the most broad in terms of resources included platform is a REACTOME[10] – a Curated Pathway Database. It is based on knowledge provided in databases as NCBI Gene, Ensembl, UniProt, UCSC Genome Browser, KEGG Compound, ChEBI, PubMed and GeneOntology [70]. Its aim is to support the research on genome and systems biology while visualizing, interpreting and analysing a pathway information. It delivers to bioinformatic community a user-friendly and intuitive tools [71]. Submitting the list of genes selected throught the final workflow, the analysis of overrepresented pathways was obtained. According to the results, the cytokine signalling in immune system and most specifically defining - signalling by Interleukins, are the most frequently assigned among the provided instances, being represented by respectively 17 and 15 entities. However, apparently there is no further pattern found – the genes involve various pathways, without special trends and preferences.

The STRING[11] is an open access database with a knowledge on protein-protein interactions and was utilized to create a visualization of a functional protein association network for a list of 72 unique genes from final selection (Figure 6.1.). Instances underlined in red are the target genes, in blue – genes further analysed as potential biomarkers. The associations are established on direct (physical) and indirect (functional) evidences. Connections are inferred from computational predictions, analogy between organisms and transferred from other (primary) data sources [72]. As could be expected, the target genes are located within the ligations in generated network, with numerous connections and interactions. This is understandable since the knowledge on those is already well established and they

[9] https://www.synapse.org/#!Synapse:syn4231880/wiki/390507; Last accessed on 26/09/2017;

[10] http://reactomerelease.oicr.on.ca/; Last accessed on 27/09/2017;

[11] https://string-db.org/; Last accessed on 27/09/2017;

share common processes related to cancer. But the point of interest are isolated cases because those hold a potential to be undiscovered tumor biomarkers. It was decided to perform an additional analysis of three genes that are not targets, that presented the highest frequency of occurence and that although appear in STRING network, they have no connection established.

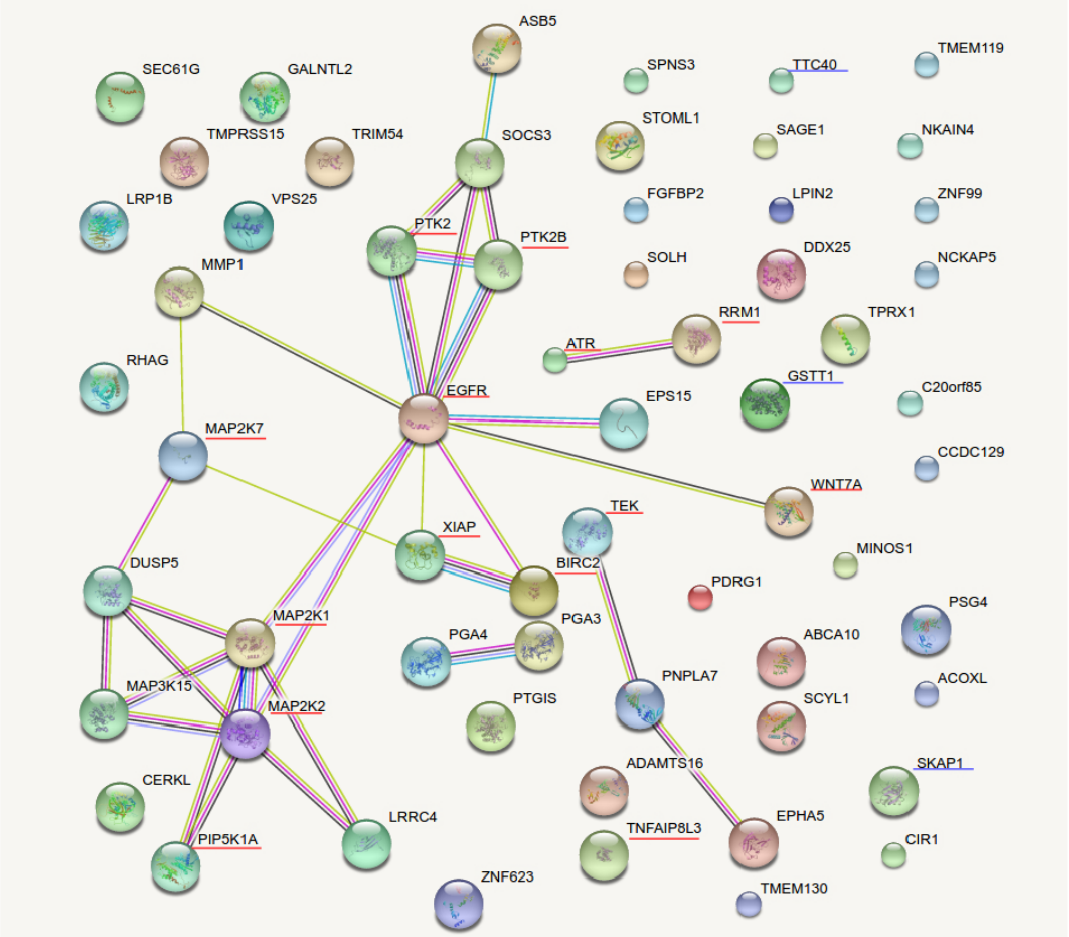

Figure 6.1. Functional protein association network created with STRING after submitting a list of 72 unique genes from final selection. Instances underlined in red are the target genes, in blue – genes further analysed as potential biomarkers.

The first of cases selected to be explored is tetratricopeptide repeat domain 40 or shortly TTC40 gene. Its mutation characteristics are indicated as informative within the selected features list. It is also known as CFAP46 - Cilia And Flagella Associated Protein 46. According to UniProtKB/Swiss-Prot it makes a part of the central apparatus of the cilium axoneme and plays a role in cilium movement. There is not much information found on this gene in the scientific literature. In a study from 2014 there was an association detected between hypermethylation of TTC40 and nasopharyngeal carcinoma. The authors identified a CpG island at 10q26.3 locus to be frequently methylated in cancer samples and to be correlated with transcriptional silencing of this previously undetermined gene [73].

TTC40 is not included in the driver gene list used in this work as described before. Since there exist among the scientific publications some indication on its association with the tumor, it may confirm the hypothesis of being a potential candidate for the cancer.

The CNV status of GSTT1 is also found to be relative to build model. This gene encodes glutathione S-transferase theta 1 protein which belongs to a family initailizing the detoxification by catalyzing the conjugation of reduced glutathione to a range of electrophilic and hydrophobic composites that are

[42] http://www.uniprot.org/; Laste accessed on 27/09/2017;

potential toxins [74]. It is located on chromosome 22q11.2 and the product enzyme is expressed in human erythrocytes. The theta class of glutathione S-transferases is associated with carcinogenesis. Particularly GSTT1 is found to contribute to larynx cancer and mutagen sensitivity related to nasopharyngeal and colorectal carcinomas (http://www.genecards.org). This gene is haplotype-specific and is referred as absent in 38% of population. The observation of GSTT1 phenotypes in a large family suggests that the gene is passed through generations according to mendelian intermediary inheritance, where due to the gene-dosage effect in the presence of 2 functional alleles the enzyme expression is doubled [75].

There are various studies indicating GSTT1 contribution to detoxification processes. Patients with nonfunctionall GSTT1 allele have frequently decreased ability to metabolize environmental and/or endogenous carcinogens or toxins and may be at risk of developing pathologies. In the work of Chen et al. [76], the GSTT1 null genotype was observed among 46% of analysed cases with myelodysplastic syndromes (MDS) while in the cancer-free controls – only among 16%. There are associations found also with occurance of aplastic anemia [77] and with reduction in birth weight among smoking mothers [78]. The explanation behind is common - a reduced capability to deal with toxic factors.

According to the references, the GSTT1 gene is a strong biomarker candidate. Its association with a cancer is broadly observed and documented but still there should be performed extra studies to confirm its predictive power.

SKAP1, Src Kinase Associated Phosphoprotein 1, is identified as informative due to its CNV status. Its product is a T cell adaptor protein that belongs to a class of intracellular compounds carrying domains with ability to recruit additional proteins [79]. Those molecules are incapable to perform any intrinsic enzymatic activity and play a role in T cell receptor and Ras signaling pathways. SKAP1 is responsible for for optimal conjugation between T-cells and antigen-presenting cells by enhancing the clustering of ITGAL integrin on the surface of T-cells. Moreover it may contribute to a high affinity immunoglobulin epsilon receptor signaling in mast cells. The only indication on the association of SKAP1 with a cancer found at this moment, is a list of dosage-sensitive cancer genes provided by CNVD and used in pre-processing of CNV data source. Thus, its potential on being a biomarker candidate requires much further investigations.

7. Conclusions

The practical aim of this project, namely the implementation of an hybrid machine learning methodology was achieved. The approach applied in the 2016 DREAM Challenge winning solution by Yuanfang Guan was explored and comprehended. As the result of this work, the functional baseline script flow reproducing the original methodology was produced using R and Python languages. Moreover, due to the optimizing manipulations, the imlementation was successfully improved providing higher evaluation scores.

Comparing a performance of different machine learning algorithms permitted gaining a practice and familiarity with the methodologies. The preferable approach for this prediction problem was identified, that is Support Vector Machine. Regarding to the merging equation, the optimization step brought improvement by the re-establishment of parameters. Although there was a trend observed among the efficiency of methods and coefficients applied, the detected variances were not critical. However, according to the common law, through the small changes the final great result may be obtained.

The feature selection procedure allowed obtaining a list of potential cancer biomarkers. Those candidates varies in the level of confidence depending in general on the information available, studies carried on the genes etc. Thus, the weaker preferably require much more profound and extended verifications, including a high number of experimental analysis.

Finally the initial aims that caused this work to arise were successfully accomplished. The process of implementation development guaranteed high training on machine learning methods, broadening the knowledge on techniques and algorithms. The approach of multi-source data integration was successfully explored opening new possibilities of application in a range of pharmacological modeling problems.

References

[1] Kannan, L., Ramos, M., Re, A., El-Hachem, N., Safikhani, Z., Gendoo, D.M.A., Davis, S., David, G.C.L., Castelo, R., Hansen, K.D., Carey, V.J., Morgan, M., Culhane, A.C., Haibe-Kains, B., Waldron, L., (2016), Public data and open source tools for multi-assay genomic investigation of disease, Briefings in Bioinformatics, 17, 603-615

[2] Hieke, S., Benner, A., Schlenl, R. F., Schumacher, M., Bullinger, L., & Binder, H., (2016), Integrating multiple molecular sources into a clinical risk prediction signature by extracting complementary information, BMC Bioinformatics, 17(1), 327

[3] Gligorijević, V. and Pržulj, N., (2015), Methods for biological data integration: perspectives and challenges, Journal of the Royal Society, Interface, 12,

[4] Rodrigues de Morais, S., (2008), A Novel Scalable and Data Efficient Feature Subset Selection Algorithm, Machine Learning and Knowledge Discovery in Databases: European Conference, ECML PKDD 2008, Antwerp, Belgium, September 15-19, 2008, Proceedings, Part II, , 298-312

[5] Peña, J.M., Nilsson, R., Björkegren, J., Tegnérab, J., (2007), Towards Scalable and Data Efficient Learningof Markov Boundaries, International Journal of Approximate Reasoning, 45(2), 211-232

[6] Nilsson, R., Peña, J.M., Björkegren, J., Tegnér, J., (2007), Consistent Feature Selection for Pattern Recognitionin Polynomial Time, The Journal of Machine Learning Research, 8, 589-612

[7] Guyon, I., Elisseeff, A., (2003), An Introduction to Variable and Feature Selection, The Journal of Machine Learning Research, 3, 1157-1182

[8] Kohavi R., John G.H., (1997), Wrappers for feature subset selection, Artificial Intelligence, 97 (1-2), 273-324

[9] Blum, A.L., Langley, P., (1997), Selection of relevant features and examples in machine learning, Artificial Intelligence, 97(1-2), 245-271

[10] AstraZeneca-Sanger Drug Combination Prediction DREAM Challenge (syn4231880), (2015), doi:10.7303/syn4231880

[11] Tan, X., Hu, L., Luquette, L.J., Gao, G., Liu, Y., Qu, H., … Elledge, S.J., (2012), Systematic Identification of Synergistic Drug Pairs Targeting HIV, Nature Biotechnology, 30(11), 1125–1130

[12] Surowiecki, J., (2006), The Wisdom of Crowds: Why the Many Are Smarter Than the Few and How Collective Wisdom Shapes Business, Economics, Societies and Nations

[13] Saez-Rodriguez, J., Costello, J.C., Friend, S.H., Kellen, M.R., Mangravite, L., Meyer, P., Norman, T. & Stolovitzky, G., (2016), Crowdsourcing biomedical research: leveraging communities as innovation engines, Nature Reviews Genetics, 17(8), 470-86

[14] Marbach, D., Costello, J.C., Küffner, R., Vega, N.M., Prill, R.J., Camacho, D.M., Allison, K.R., The DREAM5 Consortium, Kellis, M., Collins, J.J. & Stolovitzky, G., (2012), Wisdom of crowds for robust gene network inference, Nature Methods, 9, 796–804

[15] Stolovitzky, G., Monroe, D. & Califano, A., (2007), Dialogue on Reverse-Engineering Assessment and Methods, Annals of the New York Academy of Sciences, 1115(1), 1-22

[16] Green, M.R., Monti, S., Rodig, S.J., Juszczynski, P., Currie, T., O'Donnell, E., … Shipp, M.A., (2010), Integrative analysis reveals selective 9p24.1 amplification, increased PD-1 ligand expression, and further induction via JAK2 in nodular sclerosing Hodgkin lymphoma and primary mediastinal large B-cell lymphoma, Blood, 116(17), 3268–3277

[17] Fitzgerald, J. B., Schoeberl, B., Nielsen, U. B., & Sorger, P. K. , (2006), Systems biology and combination therapy in the quest for clinical efficacy., Nature chemical biology, 2, 458-466

[18] Jia, J., Zhu, F., Ma, X., Cao, Z., Cao, Z.W., Li, Y., Li, Y.X., Chen, Y.Z., (2009), Mechanisms of drug combinations: interaction and network perspectives, Nature reviews. Drug Discovery, 8(2), 111-28

[19] Synapse / Sage Bionetworks, (2015), AstraZeneca-Sanger Drug Combination Prediction DREAM Challenge / Challenge Questions. Available at https://www.synapse.org/#! Synapse:syn4231880/wiki/235650

[20] Gadagkar, S. & Call, G., (2014), Computational tools for fitting the Hill equation to dose–response curves, Journal of pharmacological and toxicological methods, 71,

[21] Gesztelyi, R., Zsuga, J., Kemeny-Beke, A., Varga, B., Juhasz, B. & Tosaki, A., (2012), The Hill equation and the origin of quantitative pharmacology, Archive for History of Exact Sciences, 66,
[22] Synapse / Sage Bionetworks, (2015), AstraZeneca-Sanger Drug Combination Prediction DREAM Challenge / Data Description. Available at https://www.synapse.org/#!Synapse:syn4231880/wiki/235651
[23] Greco, W.R., Faessel, H., Levasseur, L., (1996), The Search for Cytotoxic Synergy BetweenAnticancer Agents: a Case of Dorothy and the Ruby Slippers?, Journal of the National Cancer Institute, 88(11), 699-700
[24] Fitzgerald, J.B., Schoeberl, B., Nielsen, U.B. & Sorger, P.K. , (2006), Systems biology and combination therapy in the quest for clinical efficacy., Nature chemical biology, 2, 458-466
[25] Geary, N., (2013), Understanding synergy., American Journal of Physiology-Endocrinology and Metabolism, 304, 237-253
[26] Di Veroli, G.Y., Fornari, C., Wang, D., Mollard, S., Bramhall, J.L., Richards, F.M., & Jodrell, D.I., (2016), Combenefit: an interactive platform for the analysis and visualization of drug combinations, Bioinformatics, 32(18), 2866–2868
[27] Iorio, F., Knijnenburg, T.A., Vis, D.J., Bignell, G.R., Menden, M.P., Schubert, M., … Garnett, M.J., (2016), A Landscape of Pharmacogenomic Interactions in Cancer, Cell, 166, 740-754
[28] Gentleman, R., Carey, V., Huber, W., Irizarry, R., Dudoit, S., (2005), Bioinformatics and Computational Biology Solutions Using R and Bioconductor (Statistics for Biology and Health), , ,
[29] Irizarry, R.A., Gautier, L., Huber, W. & Bolstad, B., (2006), makecdfenv: CDF Environment Maker. R package version 1.52.0.
[30] Gautier, L., Cope, L., Bolstad, B.M. & Irizarry, R.A., (2004), affy—analysis of Affymetrix GeneChip data at the probe level, , 20, 307-315
[31] Friedman, J.H., (1991), Multivariate Adaptive Regression Splines, Ann. Statist., 19, 1-67
[32] Ye, K., Schulz, M.H., Long, Q., Apweiler, R., & Ning, Z., (2009), Pindel: a pattern growth approach to detect break points of large deletions and medium sized insertions from paired-end short reads, Bioinformatics, 25, 2865-2871
[33] Du, P., Zhang, X., Huang, C.C., Jafari, N., Kibbe, W.A., Hou, L., & Lin, S.M., (2010), Comparison of Beta-value and M-value methods for quantifying methylation levels by microarray analysis, Bioinformatics, 11
[34] Synapse / Sage Bionetworks, (2015), AstraZeneca-Sanger Drug Combination Prediction DREAM Challenge / Submitting Models. Available at https://www.synapse.org/#!Synapse:syn4231880/wiki/235659
[35] Synapse / Sage Bionetworks, (2016), Synapse / Elements of Best-performing Algorithms, , ,
[36] Barretina, J., Caponigro, G., Stransky, N., Venkatesan, K., Margolin, A.A., Kim, S., … Garraway, L.A., (2012), The Cancer Cell Line Encyclopedia enables predictive modelling of anticancer drug sensitivity, Nature, 483(7391), 603–607
[37] Goya, J., Wong, A.K., Yao, V., Krishnan, A., Homilius, M., & Troyanskaya, O.G., (2015), FNTM: a server for predicting functional networks of tissues in mouse, Nucleic Acids Research, 43(Web Server issue), W182–W187
[38] Guan, Y., Myers, C.L., Lu, R., Lemischk , I.R., Bult, C.J., et al., (2008), A Genomewide Functional Network for the Laboratory Mouse, PLOS Computational Biology, 4,
[39] Guan, Y., (2016), GuanLab's solution to the 2016 AstraZeneca-Sanger Drug Combination Prediction DREAM Challenge, Synapse Repository, Synapse ID: syn5614689,
[40] Kulis, M., Esteller, M., (2010), DNA methylation and cancer, Advances in Genetics, 70, 27-56
[41] Ehrlich, M., (2009), DNA hypomethylation in cancer cells, Epigenomics, 1(2), 239-259
[42] MathWorks, (Accessed June 21, 2017), MathWorks / Documentation: TreeBagger. Available at https://www.mathworks.com/
[43] Python Software Foundation, (Accessed June 21, 2017), Python Language Reference, version 2.7. Available at http://www.python.org
[44] Burns, P., (Accessed June 21, 2017), Burn Statistics Tutorial: Why use the R Language? Available at http://www.burns-stat.com

[45] Ho, T.K., (1995), Random Decision Forests, Proceedings of the Third International Conference on Document Analysis and Recognition (Volume 1), , 278
[46] Breiman, L., (2001), Random Forests, Machine Learning, 45, 5-32
[47] Amit, Y., Geman, D., (1997), Shape Quantization And Recognition With Randomized Trees., Neural Computation, 9, 1545-1588
[48] Rubio-Perez, C., Tamborero, D., Schroeder, M.P., Antolín, A.A., Deu-Pons, J., Perez-Llamas, C., Mestres, J., Gonzalez-Perez, A., Lopez-Bigas, N., (2015), In silico prescription of anticancer drugs to cohorts of 28 tumor types reveals novel targeting opportunities., Cancer Cell, 27, 382-396
[49] Gonzalez-Perez, A., Perez-Llamas, C., Deu-Pons, J., Tamborero, D., Schroeder, M.P., Jene-Sanz, A., Santos, A. & Lopez-Bigas, N., (2013), IntOGen-mutations identifies cancer drivers across tumor types, Nature Methods, 10, 1081-1082
[50] Tamborero, D., Rubio-Perez, C., Deu-Pons, J., Schroeder, M., Vivancos, A., Rovira, A., Tusquets, I., Albanell, J., Rodon, J., Tabernero, J., Dienstmann, R., Gonzalez-Perez, A. & Lopez-Bigas, N. , (2017), Cancer Genome Interpreter Annotates The Biological And Clinical Relevance Of Tumor Alterations, bioRxiv
[51] Qiu, F., Xu, Y., Li, K., Li, Z., Liu, Y. Duanmu, H., Zhang, S., Li, Z., Chang, Z., Zhou, Y., Zhang, R., Zhang, S., Li, C., Zhang, Y., Liu, M., Li, X., (2012), CNVD: Text mining-based copy number variation in disease database., Human Mutation, 33, 2375-2381
[52] Breiman, L., Cutler, A., Liaw, A. & Wiener, M., (2015), randomForest: Breiman and Cutler's Random Forests for Classification and Regression, CRAN Repository
[53] Matthews, B.W., (1975), Comparison of the predicted and observed secondary structure of T4 phage lysozyme, Biochimica et Biophysica Acta (BBA) - Protein Structure, 405(2), 442-451
[54] Powers, D.M.W., (2011), Evaluation: From Precision, Recall and F-Measure to ROC, Informedness, Markedness & Correlation, Journal of Machine Learning Technologies, 2(1), 37-63
[55] Brodersen, K.H., Ong, C.S., Stephan, K.E. & Buhmann, J.M., (2010), The balanced accuracy and its posterior distribution, Pattern Recognition, International Conference
[56] Tibshirani, R., (1996), Regression Shrinkage and Selectionvia the Lasso, Journal of the Royal Statistical Society. Series B (Methodological), 58, 267-288
[57] Kursa, M.B., Rudnicki, W.R., (2017), Package 'Boruta': Wrapper Algorithm for All Relevant Feature Selection, CRAN Repository
[58] Kursa, Miron B., Rudnicki, Witold R., (2010), Feature Selection with the Boruta Package, Journal of Statistical Software, 36, 1-13
[59] Friedman, J., Hastie, T., Simon, N., Qian, J., Tibshirani, R. , (2017),
[60] Cortes, C. & Vapnik, V., (1995), Support-vector network, , 20, 1-25
[61] Burges, C.J.C., (1998), A Tutorial on Support Vector Machines for PatternRecognition, Data Mining and Knowledge Discovery, 2, 121-167
[62] Dudek, A.Z., Arodz, T., Gálvez J., (2006), Computational Methods in Developing Quantitative Structure-Activity Relationships (QSAR): A Review, Combinatorial chemistry & high throughput screening, 9, 213-28
[63] Friedman, J., (1991), Multivariate Adaptive Regression Splines, 1-141
[64] Zhang, W. & Go, A.T.C., (2016), Multivariate adaptive regression splines and neural network models for prediction of pile drivability, Geoscience Frontiers, 7, 45-52
[65] StatSoft, Inc., (2013), Electronic Statistics Textbook. Multivariate Adaptive Regression Splines (MARSplines). Available at http://www.statsoft.com/textbook/
[66] Meyer, D., Dimitriadou, E., Hornik, K., Weingessel, A., Leisch, F., Chang, C., Lin, C. , (2017),
[67] Chang, C.C., Lin, C.J., (2011), LIBSVM: a library for support vector machines, 27:1 -- 27:27
[68] Milborrow, S., Hastie, T. & Tibshirani, R., (2011), earth: Multivariate Adaptive Regression Splines [R package earth version 4.5.1]
[69] J. Friedman, (1991), Multivariate Adaptive Regression Splines, 1-141
[70] Croft, D., Mundo, A.F., Haw, R., Milacic, M., Weiser, J., Wu, G., … D'Eustachio, P., (2014), The Reactome pathway knowledgebase, Nucleic Acids Research, 42, D472–D477

[71] Fabregat, A., Sidiropoulos, K., Garapati, P., Gillespie, M., Hausmann, K., Haw, R., … D'Eustachio, P., (2016), The Reactome pathway Knowledgebase, Nucleic Acids Research, 44, D481–D487
[72] Jensen, L.J., Kuhn, M., Stark, M., Chaffron, S., Creevey, C., Muller, J., … von Mering, C., (2009), STRING 8—a global view on proteins and their functional interactions in 630 organisms, Nucleic Acids Research, 37, 412-416
[73] Ayadi, W., Allaya, N., Frikha, H., Trigui, E., Khabir, A., Ghorbel, A., … Mokdad-Gargouri, R. , (2014), Identification of a Novel Methylated Gene in Nasopharyngeal Carcinoma: TTC40, BioMed Research International
[74] Pemble, S., Schroeder, K. R., Spencer, S. R., Meyer, D. J., Hallier, E., Bolt, H. M., Ketterer, B., Taylor, J. B., (1994), Human glutathione S-transferase theta (GSTT1): cDNA cloning and the characterization of a genetic polymorphism, Biochemical Journal, 300, 271-276
[75] Wiebel, F.A., Dommermuth, A., Thier, R., (1999), The hereditary transmission of the glutathione transferase hGSTT1-1 conjugator phenotype in a large family, Pharmacogenetics, 9, 251-256
[76] Chen, H., Sandler, D.P., Taylor, J.A., Shore, D.L., Liu, E., Bloomfield, C.D., Bell, D.A., (1996), Increased risk for myelodysplastic syndromes in individuals with glutathione transferase theta 1 (GSTT1) gene defect, Lancet, 347, 295-297
[77] Lee, K.A., Kim, S.H., Woo, H.Y., Hong, Y.J., Cho, H.C., (2001), Increased frequencies of glutathione S-transferase (GSTM1 and GSTT1) gene deletions in Korean patients with acquired aplastic anemia, Blood, 98, 3483-3485
[78] Wang, X., Zuckerman, B., Pearson, C., Kaufman, G., Chen, C., Wang, G., Niu, T., Wise, P.H., Bauchner, H., Xu, X., (2002), Maternal cigarette smoking, metabolic gene polymorphism, and infant birth weight, JAMA, 287, 195-202
[79] Raab, M., Smith, X., Matthess, Y., Strebhardt, K., Rudd, C.E., (2011), SKAP1 protein PH domain determines RapL membrane localization and Rap1 protein complex formation for T cell receptor (TCR) activation of LFA-1, The Journal of Biological Chemistry, 286, 29663-70

Appendix 1

Specification of the files

This appendix provides tables presenting structure of the files organizing a data used in this work.

A. Pharmacological Data

The following table reflects the structure of the *.csv* file recording pharmacological data.

Column name	***Data type***	***Description and comments on nomenclature***	***Example***
CELL_LINE	Factor	Unique and common normalised cell line identifier;	BT-20
COMPOUND_A	Factor	Unique and anonymised drug A identifier; Name indicates primary target of action and specifies the version of pharmaceutical;	AKT
COMPOUND_B	Factor	Unique and anonymised drug B identifier; Name indicates primary target of action and specifies the version of pharmaceutical;	ADAM17
MAX_CONC_A	Numeric	The maximum concentration of compound A tested in experiments; Expressed in μM;	1
MAX_CONC_B	Numeric	The maximum concentration of compound B tested in experiments; Expressed in μM;	75
IC50_A	Numeric	The concentration of compound A causing 50% of the maximum cell death; Expressed in μM;	1
H_A	Numeric	The slope of the curve fit (Hill model) for compound A	0.8090022
Einf_A	Numeric	Maximum cells killed obtained with compound A; Expressed in percentage;	59.1224363
IC50_B	Numeric	The concentration of compound B causing 50% of the maximum cell death; Expressed in μM;	9.63971363
H_B	Numeric	The slope of the curve fit (Hill model) for compound B	0.7579769
Einf_B	Numeric	Maximum cells killed obtained with compound B; Expressed in percentage;	91.5934245
SYNERGY_SCORE	Numeric	Computed total synergy score for A- B drug pair and cell line combination	29.54039
QA	Numeric	Quality Assesment; ‘0’ for assay with missing data; ‘-1’ for assay with ≥ 1 record of cell kill above 125%; ‘-2’ for assay with ≥ 1 record of cell kill below -10%; ‘-3’ for the assay with the difference between smoothed and non-smoothed fit above 25%; ‘1’ for assay for which no abnormalities were detected;	1
COMBINATION_ID	Factor	The identifier of drug pair; Name combining the identifiers of drug A and B, joining them by ’.’ in alphabetical order;	ADAM17.AKT

B. Copy Number Variants Data

The following table reflects the structure of the *.csv* file recording data on CNVs.

Column name	***Data type***	***Description and comments on nomenclature***	***Example***
cell_line_name	Factor	Unique and common normalised cell line identifier;	22RV1
gene	Factor	Normalised gene identifier, according to COSMIC annotation (mostly equivalent to HGNC nomenclature);	ZZZ3
chr_GRCh38	Factor	Chromosomal localization of CNV according to GRCh38;	1
gene_start_GRCh38	Numeric	Coordinates of the gene's start according to GRCh38;	7756565
gene_end_GRCh38	Numeric	Coordinates of the gene's stop according to GRCh38;	7763335
max_cn_GRCh38	Numeric	Maximum number of copies of gene (the coding sequence) found within the genome; '-' for unknown values; '-1' for undetermined value;	2
min_cn_GRCh38	Numeric	Minimum number of copies of gene (the coding sequence) found within the genome; '-' for unknown values; '-1' for undetermined value;	2
zygosity_GRCh38	Factor	Identifies if the copies of gene sequence are continuous or interrupted; 'D' for the copied sequence encompassing > 1 genomic segment; '-' for the copies identified wihin the single genomic segment;	H
disruption_status	Factor	Determines if alleles are equal or different;'H' for heterozygous repetitions; 'L' for any occurance of LOH (loss of heterozygosity) ; '0' for the total homozygous deletion;	D

C. DNA Sequencing Data

The following table reflects the structure of the *.csv* file recording data on mutations.

Column name	***Data type***	***Description and comments on nomenclature***	***Example***
Gene.name	Factor	Normalised gene identifier; According to COSMIC annotation (mostly equivalent to HGNC nomenclature);	CTNNB1
Accession.Number	Factor	Unique identifier of transcript; According to Ensembl norms;	ENST00000349496
Gene.CDS.length	Numeric	Length of the gene; The unit used: base pair;	2346
HGNC.ID	Numeric	Standarized identifier of gene (if exists); According to the HUGO Gene Nomenclature Committee norms;	2514
cell_line_name	Factor	Unique and common normalised cell line identifier;	SW48
ID_sample	Numeric	Unique identifier of sample; According to COSMIC identification standards;	909751
ID_tumour	Numeric	Unique identifier of tumour; According to COSMIC identification standards;	827235
Primary.site	Factor	The type of sample’s tissue of origin; According to COSMIC identification standards;	large_intestine
Site.subtype	Factor	The subtype of the sample’s tissue of origin; According to COSMIC identification standards; According to COSMIC identification standards;	colon
Primary.histology	Factor	The type of sample’s tissue of origin; According to histological classification norms;	carcinoma
Histology.subtype	Factor	The subtype of the sample’s tissue of origin; According to histological classification norms;	adenocarcinoma
Genome.wide.screen	Logical	Identifies if the mutation comes from wide genome/exome sequencing study	y
Mutation.ID	Factor	Unique mutation identifier (according to COSMIC classification standard)	COSM5673
Mutation.CDS	Factor	The specification of the mutation on the nucleotide level; The notation accoring to the standards of the Human Genome Variation Society;	c.98C>A
Mutation.AA	Factor	The specification of the change on the peptide level provoked by the mutation; The notation accoring to the standards of the Human Genome Variation Society;	p.533Y
Mutation.Description	Factor	The specification of the type of mutation; Among others: insertion, deletion, substitution, complex etc.	Substitution – Missense
Mutation.zygosity	Factor	The status of zygosity of mutation; 'het’ for mutations reported as heterozygous; ‘hom’ for mutations reported as homozygous;	het

GRCh	Numeric	Specification of the reference human genome build; '37' for GRCh37/Hg19; '38' for GRCh38/Hg38;	38
Mutation.Genome.position	Factor	The coordinates of mutations defining localization ath the genome	3:412240-412246
strand	Factor	Orientation of the strand; '+' for positive/forward/sense strand; '-' for negative/reverse/antisense strand;	+
SNP	Factor	Identifies if mutation is recognized as SNP; 'y' for SNPs recognized within the 1000 genomes project; 'n' for apparently neutral SNPs according to dbSNP and to a panel of 378 normal (non-cancer) samples from Sanger CGP sequencing;	n
FATHMM.prediction	Factor	FATHMM (Functional Analysis through Hidden Markov Models) descriptor defining pathogenicity of mutation; 'Cancer' or 'Damaging' for mutations considered as pathogenic; 'Passenger', 'Tolerated' or 'Others' for apparently neutral mutations;	CANCER
Mutation.Somatic.status	Factor	The specification of the evidence on somatic status of the mutation; 'Confirmed somatic variant' for mutation experimentally vlidated to be somatic in cancer and control cells; 'Reported in another cancer sample as somatic' when the experimental validation did not provide an evidence but the mutation was reported in the literature as somatic; 'Variant of unknown origin' for a mutation that was verified to be somatic solely in the tumour sample;	Confirmed somatic variant
Pubmed_PMID	Numeric	The identifier corresponding to the publications involving the sample; According to PUBMED annotation;	NA
ID_STUDY	Numeric	The identifiers of studies engaging the sample	NA
Institute	Factor	The unit providing the sample	American Type Culture Collection
Institute.Address	Factor	Address of the unit providing the sample	P.O. Box 19, Manassas, USA
Catalogue.Number	Factor	Internal identifier of the sample assigned in the unit	CCL-231
Sample.source	Factor	The biological origin of the sample collected	Cell-line
Tumour.origin	Factor	The specification of the neoplastic origin of the collected sample; 'primary' for the sample collected at the anatomical site of tumour outset; 'metastasis' for the sample collected at the secondary localizations, different than where the tumour progression began ; 'NS' for not specified origin;	primary
Age	Numeric	Age of the individual	82
Comments	Factor	Additional information related to sample	Grade:II,Stage:II

D. Compound Data

The following table reflects the structure of the .txt file listening the chemical and structural characteristics of 119 unique compounds.

Column name	*Data type*	*Description and comments on nomenclature*	*Example*
ChallengeName	Factor	Unique and anonymised drug A identifier; Name indicates primary target of action and specifies the version of pharmaceutical;	Carboplatin
Target (Official Symbol)	Factor	List of all putative targets; Gene names according to the HGNC annotation;	DNA
HBA	Numeric	H-bond acceptors; The number of oxygen and nitrogen atoms; Indicates polarity of chemical;	6
cLogP	Numeric	Calculated octanol-water partition coefficient; Determines solubility of the chemical;	-2.34
HBD	Numeric	H-bond donors; The number of groups -NH or -OH carring extra hydrogen atom; Indicates polarity of chemical;	4
Lipinski	Numeric	Lipinski rule of 5: The number of fulfilled rules among: HBA ≤ 10, HBD ≤ 5, cLogP ≤ 5 and MW < 500 Da ; Determines drug-likeliness of chemical;	0
SMILES or PubChem ID	Factor	The additional compound specification (if available); According to the Simplified Molecular Input Line Entry Specification (SMILES) or to PubChem annotation;	C1CC2(C1)C(=O)O[Pt](OC2=O)(N)N
MW	Numeric	Molecular weight; Expressed in g/mol;	369.2

E. Driver Genes Data

The following table reflects the structure of the *.csv* file listening the 498 cancer drivers and their characteristics downloaded from IntOGen platform.

Column name	***Data type***	***Description and comments on nomenclature***	***Example***
geneHGNCsymbol	Factor	Gene names according to the HGNC annotation;	ABL2
Driver_type	Factor	Specification of alteration type; ‘CNA’ for Copy Number Alteration ; ‘FUSION’ for hybrid gene formed from previously separated genes; ‘MUTATION’ for permanent alteration of the nucleotide sequence;	FUSION
Role	Factor	The effect of the gene alteration; ‘A’ for altered gene product that acts antagonistically to the wild-type allele; ‘Activating’ for enhancement of the effect of a gene product; ‘Loss of function’ for activity reduction or total inactivation of a gene product; ‘No class’ for unknown role of the alteration;	Activating
OncodriveROLE_prob	Numeric	Probability of the identified driver role;	0.877

F. Copy Number Variations in Disease Data

The following table reflects the structure of the *.txt* filedata on CNVs associated with cancer downloaded from CNVD platform.

Column name	***Data type***	***Description and comments on nomenclature***	***Example***
CNVD_ID	Numeric	Unique identifier according to the CNVD standard;	302652
Species	Factor	The organism in the study;	Homo sapiens
Chromosome	Factor	Chromosomal localization of CNV;	16
Start_Position	Numeric	Coordinates of the CNV’s start;	88280576
End_Position	Numeric	Coordinates of the CNV’s stop;	88290263
Chr_region	Factor	Coordinates of the chromosome region with CNV;	16q24
Describe	Factor	Specification of the CNV type;	Insertion
Gene	Factor	Genes encompassed by CNV, according to the HGNC nomenclature;	CDK10
Disease	Factor	Disease associated with CNV;	Gastric cancer
Platform	Factor	Specification of the platform used in the study;	Array CGH
Sample	Factor	Specifications on samples in study (number and type)	183 primary gastric cancer
quency	Numeric	Ratio of CNV observations among total number of samples;	0.18
PubMed_ID	Numeric	Study reference; According to PUBMED annotation;	24379144

Appendix 2

Selected Features

This appendix provides an list of genes selected with a developed workflow using the Lasso algorithm. Instances are ordered according to the frequency of occurance, starting from the most recurrent.

List of Genes:

ATR
EGFR
DUSP5
PIP5K1A
TTC40
BIRC2
LOC100507266
GSTT1
LRRC4
TNFAIP8L3
MAP2K7
SKAP1
MAP2K1
XIAP
LRP1B
C7orf54
NCKAP5
PNPLA7
PSG4
SEC61G
ACOXL
SAGE1
CES1P1
CIR1
NKAIN4
TPRX1
WNT7A
ABCA10
ASB5
CCDC129

CCDC129ENST00000451887
RHAG
SPNS3
C20orf85
DDX25
GALNTL2
MAP2K2
PGA3
PTK2
ZNF99
TRIM54
PTGIS
SOCS3
SOLH
STOML1
MYOFENST00000371501
SCYL1ENST00000270176
TMEM119
VPS25
ADAMTS16
CERKL
ELK2AP
LOC283922
MAP3K15
MMP1
PGA4
RRM1
ZNF623
LPIN2
PDRG1
TEK
PTK2B
TPTE2P6
EPS15
MINOS1
TMEM130
EPHA5
FGFBP2
HLA.DPB1
HTR7ENST00000371721
SCYL1
TMPRSS15